

New Aminoimidazoles as β -Secretase (BACE-1) Inhibitors Showing Amyloid- β ($A\beta$) Lowering in Brain

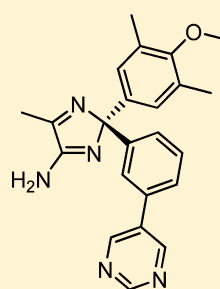
Ylva Gravenfors,^{*,†} Jenny Viklund,[†] Jan Blid,[†] Tobias Ginman,[†] Sofia Karlström,[†] Jacob Kihlström,[†] Karin Kolmodin,[†] Johan Lindström,[†] Stefan von Berg,[†] Fredrik von Kieseritzky,[†] Can Slivo,[†] Britt-Marie Swahn,[†] Lise-Lotte Olsson,^{||} Patrik Johansson,^{||} Susanna Eketjäll,[‡] Johanna Fälting,[‡] Fredrik Jeppsson,[‡] Kia Strömberg,[‡] Juliette Janson,[§] and Fredrik Rahm^{†,⊥}

[†]Department of Medicinal Chemistry, [‡]Department of Neuroscience, and [§]Department of DMPK, AstraZeneca R&D Södertälje, SE-151 85 Södertälje, Sweden

^{||}Discovery Sciences, AstraZeneca R&D Mölndal, SE-431 83 Mölndal, Sweden

S Supporting Information

ABSTRACT: Amino-2*H*-imidazoles are described as a new class of BACE-1 inhibitors for the treatment of Alzheimer's disease. Synthetic methods, crystal structures, and structure–activity relationships for target activity, permeability, and hERG activity are reported and discussed. Compound (S)-**1m** was one of the most promising compounds in this report, with high potency in the cellular assay and a good overall profile. When guinea pigs were treated with compound (S)-**1m**, a concentration and time dependent decrease in $A\beta_{40}$ and $A\beta_{42}$ levels in plasma, brain, and CSF was observed. The maximum reduction of brain $A\beta$ was 40–50%, 1.5 h after oral dosing (100 μ mol/kg). The results presented highlight the potential of this new class of BACE-1 inhibitors with good target potency and with low effect on hERG, in combination with a fair CNS exposure in vivo.



(S)-**1m**

BACE-1 IC ₅₀	24 nM
hERG IC ₅₀	>33 μ M
Brain $A\beta$ lowering	40–50% [100 μ mol/kg p.o.]

■ INTRODUCTION

Collected statistics regarding Alzheimer's disease (AD) predict a negative socioeconomic effect from the increasing number of AD patients via growth in the aging population.^{1,2} The drug therapies available today treat the symptoms and do not address the underlying neuropathology.² There is a huge need for research in the area to find treatments to prevent or halt the progression of the disease.

During the progression of AD, neurons degenerate, leading to significant shrinkage of the brain and an imbalance of the different neurotransmitters. In post-mortem AD brains, insoluble proteins in the form of plaques and tangles are accumulated.^{3,4} The plaques contain amyloid- β peptide ($A\beta$), generated from proteolytic cleavage of amyloid precursor protein (APP).⁵ The first step in the processing of APP to generate $A\beta$ is cleavage by the aspartyl protease β -secretase, or BACE-1 (β -site APP cleaving enzyme).^{6–10} This step is followed by γ -secretase cleavage, resulting in $A\beta$ of different lengths. One form of the degradation product, $A\beta_{42}$, is thought to be particularly pathogenic. Early onset AD is associated with genetic alterations in presenilin-1 (PS1, part of the γ -secretase complex) and APP, which implicates the amyloid pathway and alterations in the production of $A\beta$ as important for disease.¹¹ The BACE-1 homologue BACE-2 is expressed at very low levels in neurons, and a role of BACE-2 in APP processing or contributing to disease remains uncertain.⁸ Taken together, these data indicate that BACE-1 inhibition, to stop or reduce

the production of $A\beta$, is an attractive approach to modify Alzheimer's disease.^{5,12}

Despite extensive research, the identification of a potent BACE-1 inhibitor, efficacious in man, has proven to be a challenge.^{13–15} Two main structural classes of BACE-1 inhibitors are described in the literature: transition state isosteres of the peptide substrate^{16,17} and smaller cyclic structures with an amidine or guanidine moiety, interacting with the two catalytic aspartates of BACE-1.^{18–23} The substrate transition state isosteres give potent inhibitors but have often had limitations in physicochemical properties being large, flexible, and polar. However, this compound class was developed into hydroxyethylamine isosteres that have recently achieved brain $A\beta$ lowering in animal models.^{24,25} One compound in this family of BACE-1 inhibitors has shown cognitive performance improvement in transgenic mice after subcutaneous administration.²⁶ BACE-1 inhibitors containing an amidine or guanidine moiety have been identified from fragment-based or high throughput screens.^{18,20,22,23,27} These compounds have, after extensive optimization, shown brain $A\beta$ lowering in animal models^{22,28} and CSF $A\beta$ -reduction in rat²³ or humans.²⁰ Another BACE-1 inhibitor, from a different structural class, has shown cognition improvement in mice and

Special Issue: Alzheimer's Disease

Received: July 9, 2012

Published: September 27, 2012

rat.^{29,30} However, disease modification from BACE-1 inhibition in humans is still not reported.

During our in-house research in developing BACE-1 inhibitors, we have investigated different amidine-containing structures of the types depicted in Figure 1.^{19,22,27} Although

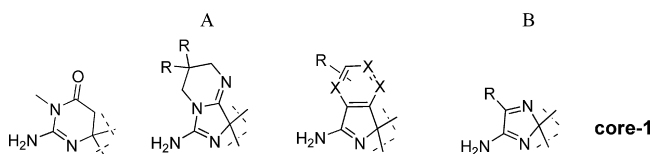


Figure 1. (A) Examples of cyclic amidine cores of BACE-1 inhibitors previously investigated in-house: dihydroisocytosines, bicyclic aminoimidazoles, and aminoisindoles ($X = \text{CH}, \text{CR},$ or N). (B) Amino-2*H*-imidazole, **core-1**.

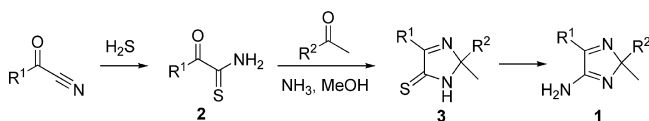
these structural classes share the same chemical motif important for BACE-1 inhibition, they have different physicochemical properties, and thus some chemical series have been more permeable and less susceptible to efflux than others.^{19,22} A low efflux has been shown to be most important to achieve brain exposure in vivo.³¹ In addition, the generic pharmacophore of many of the described BACE-1 inhibitors, which feature a basic functionality and two to four aromatic rings, overlaps with published pharmacophores of the human ether-a-go-go-related gene (hERG) encoded potassium ion channel,^{32–34} and we have reported inhibitory values.²²

Part of our strategy was to look into modifications of the amidine-containing core structure in order to investigate if new BACE-1 inhibitors with different profiles could be discovered. Amino-2*H*-imidazole (**core-1**, Figure 1) is differentiated from the earlier reported cores with regard to polarity and size, factors that could influence target potency, permeability, and hERG activity. The aim of this work was to evaluate **core-1** by investigating the profiles of analogues from this core, with respect to the above-mentioned properties. We will discuss the synthesis, SAR, and the first in vivo studies of this new class of BACE-1 inhibitors.

SYNTHESIS

The first reported synthesis of the amino-2*H*-imidazole **core-1** was described by Asinger in 1963.³⁵ The amino-2*H*-imidazoles were formed as a byproduct during the synthesis of imidazothiones **3**, which were efficiently prepared by a sequential synthesis, as described in Scheme 1.³⁶

Scheme 1. First Practical Synthesis of Amino-2*H*-imidazole Precursor **3**



On the basis of the synthetic method illustrated above and a similar procedure also described by Asinger,³⁷ new routes (methods A, B, and C) were developed for synthesizing the various amino-2*H*-imidazoles **1** (Scheme 2).^{38,39} The methods of preparation for compounds **1a–t** are summarized in Table 1 (for **1u** and **1v**, see Figure 2).

RESULTS AND DISCUSSION

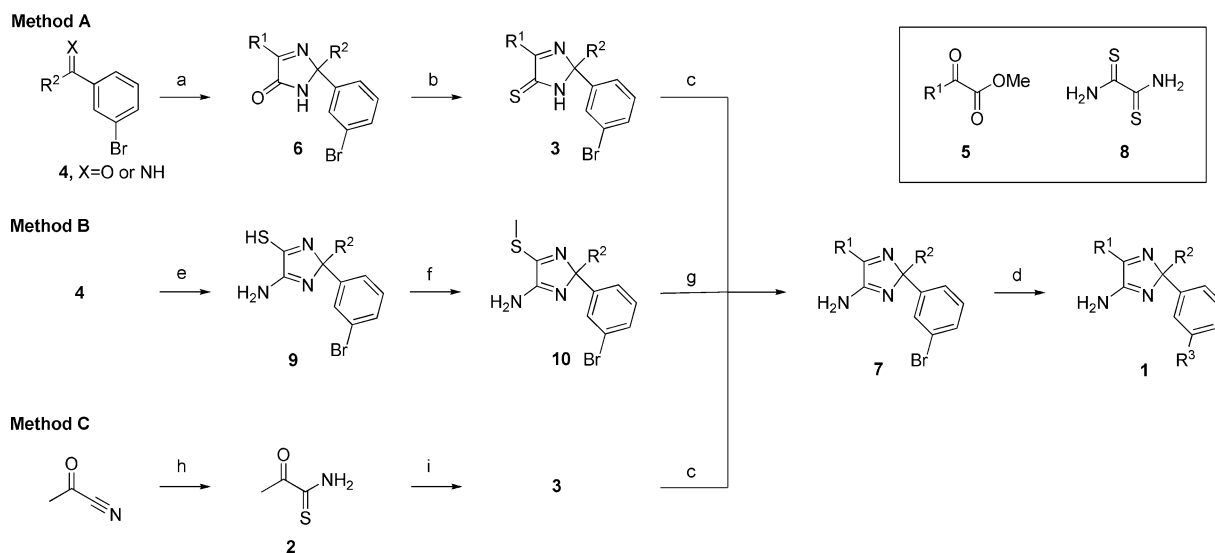
Compounds **1a–v** were evaluated for BACE-1 inhibition in one enzymatic and one cellular assay (hBACE-1, TR-FRET, and SH-SY5Y sAPP β release assays, respectively). The cell-based assay for BACE-1 inhibition used specific antibodies to monitor reduction of sAPP β release from human neuronal-derived SH-SY5Y cells. Other measured properties were permeability estimations ($P_{\text{app}}(\text{A} \rightarrow \text{B})$ values and efflux classifications), hERG activity, pK_a values, lipophilicity (experimentally determined as an estimated $\log D$ value⁴⁰), and aqueous solubility. The efflux of the compounds was measured in MDCK-MDR1 cells to estimate P-gp-mediated transport. The compounds are classified depending on their measured efflux values, as low (efflux ratio of <2.5), medium, or high (efflux ratio of >3.5). All data together with some calculated values are reported in Tables 2–4.

The first synthesized amino-2*H*-imidazoles **1a** ($R^1 = \text{Ph}$) and **1b** ($R^1 = \text{isopropyl}$) did not show any, or showed very little, activity in the TR-FRET assay (no IC_{50} could be derived). When the size of R^1 was decreased, as for **1c** and **1d** ($R^1 = \text{Me}$), IC_{50} values were measured as 3.5 and 13 μM , respectively (Table 2). The pK_a values of these compounds were measured as 6.5 and 6.7, respectively, which is within a range that has been reported to yield active compounds for BACE-1 inhibition.⁸ Addition of aryls as R^2 -substituents (**1e–k**) gave the first compounds with submicromolar potencies in the TR-FRET assay. A small substituent as R^1 was beneficial for BACE-1 inhibition (compare **1f** and **1j**). As previously reported for compounds with an acceptor motif reaching out toward Trp76,¹⁸ potency increased, and the combination of a methyl as R^1 together with a larger R^2 showed promising biochemical data, e.g., **1h** ($\text{IC}_{50} = 0.17 \mu\text{M}$; ligand efficiency,⁴³ $\text{LE} = 0.34$) and **1j** ($\text{IC}_{50} = 0.27 \mu\text{M}$; $\text{LE} = 0.33$). By stepwise introduction of methyl groups in the 3 and 5 positions in which R^2 is 4-methoxyphenyl (from **1j** to **1l** and **1m**), we observed a 3-fold increase in potency for each methyl group, both in the TR-FRET and in the SH-SY5Y assay.

To further improve interaction with the protein, we hypothesized that an alkyne moiety, on the aromatic ring in R^3 , could expand into the S3sp (S3 subpocket).²² There was a clear increase in potency in the cellular assay for **1n** in comparison with **1m**.

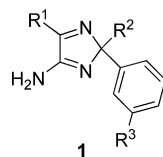
Compounds **1h–l** were more potent in the TR-FRET assay than compound **1g**, although this gain in potency in the biochemical assay for **1h–k** (though not **1l**) was not observed in the cellular assay. This difference between enzymatic and cellular potency has been observed before^{19,46} and is reported to be correlated to the pK_a of the inhibitors. Indeed, the pK_a values for the compounds with R^2 -aryl were reduced 1 log unit compared to the early R^2 -methyl (**1d**, $\text{pK}_a = 6.7$ and **1k**, $\text{pK}_a = 5.7$), which we hypothesized to have caused this reduction in cellular potency.

As reported in Table 2, the compounds with aryls in R^2 showed a good hERG profile with most compounds inactive at the highest concentration tested (33 μM). A matched pair analysis between compound **1j** (hERG $\text{IC}_{50} > 33 \mu\text{M}$) and 4-fluoro-1-(4-methoxyphenyl)-1-(3-(pyrimidin-5-yl)phenyl)-1*H*-isindol-3-amine²² (hERG $\text{IC}_{50} = 0.5 \mu\text{M}$) from an earlier published series shows that compound **1j** is more than 65 times less prone to interact with this potassium channel. The weak interaction with hERG could be explained by the decreased lipophilicity and pK_a ($\text{ElogD} = 1.1$ and $\text{pK}_a = 5.2$ for **1j**,

Scheme 2. Various Methods for Preparing Amino-2H-imidazoles 1^a

^aReagents and conditions: (a) 5, 7 M NH₃ in methanol, 120 °C; (b) P₂S₅, pyridine; (c) *t*-BuOOH, NH₃; (d) boronic acid or stannane reactant, Pd catalyst; (e) ethanebis(thioamide) 8, 7 M NH₃ in methanol; (f) MeI, THF; (g) MeMgBr, ZnI₂, cat. Pd₂Cl₂(PPh₃)₂, THF or MeMgBr, cat. Ni(dppp)Cl₂, PhMe; (h) H₂S, Et₃N, 2-methyl THF; (i) 4, if X = O, 7 M NH₃ in methanol or if X = NH, methanol.

Table 1. Synthesized Amino-2H-imidazoles, 1



product	method	R ¹	R ²	R ³
1a	A ^a	Ph	Me	pyridin-3-yl
1b	A	<i>i</i> -Pr	Me	pyridin-3-yl
1c	A	Me	Me	3-methoxyphenyl
1d	A	Me	Me	pyridin-3-yl
1e	A	<i>i</i> -Pr	Ph	pyrimidin-5-yl
1f	A	<i>i</i> -Pr	4-methoxyphenyl	pyrimidin-5-yl
1g	A	Me	Ph	pyridin-3-yl
1h	A	Me	pyridin-4-yl	3-methoxyphenyl
1i	B	Me	4-fluorophenyl	pyridin-3-yl
1j	B	Me	4-methoxyphenyl	pyrimidin-5-yl
1k	B	Me	4-methoxyphenyl	pyridin-3-yl
1l	C	Me	3-methyl-4-methoxyphenyl	pyrimidin-5-yl
1m	B	Me	3,5-dimethyl-4-methoxyphenyl	pyrimidin-5-yl
1n	C	Me	3,5-dimethyl-4-methoxyphenyl	5-(prop-1-ynyl)pyridin-3-yl
1o	B	Me	benzyl	pyrimidin-5-yl
1p	C	Me	cyclopropyl	5-chloropyridin-3-yl
1q	B	Me	cyclohexyl	pyridin-3-yl
1r	B	Me	tetrahydro-2H-pyran-4-yl	3-methoxyphenyl
1s	B	Me	4-acylpiperidin-4-yl	3-methoxyphenyl
1t	C	Me	cyclopropyl	5-(prop-1-ynyl)pyridin-3-yl

^a1a was prepared by a slightly altered procedure; see Supporting Information.

compared to ElogD = 2.4 and pK_a = 8.2 for 4-fluoro-1-(4-methoxyphenyl)-1-(3-(pyrimidin-5-yl)phenyl)-1H-isindol-3-amine).^{22,47}

The Caco-2 permeability for the compounds was good, with P_{app}(A→B) values ranging from 12 × 10⁻⁶ to 41 × 10⁻⁶ cm/s. However, the P-glycoprotein (P-gp) mediated efflux values (as determined with the in vitro MDCK-MDR1, ABBA cell assay) were classified as medium or high, for most of the compounds

tested (Table 2). One reason for the good Caco-2 permeability could be the relatively low pK_a of the compounds, leading to a higher percentage of uncharged molecules at physiological pH.^{42,43}

One of the most promising compounds was 1m, showing a good overall profile. The enantiomers of compound 1m were separated and profiled, and it became clear that the S-enantiomer was primarily responsible for the BACE-1

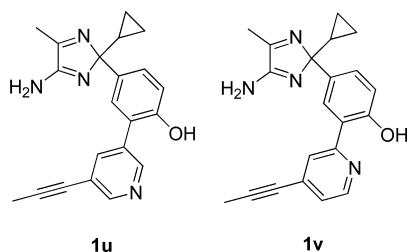


Figure 2. Amino-2*H*-imidazoles **1u** and **1v** were prepared using method C (see Experimental Section).

inhibition. Compound (*S*)-**1m** achieved potencies of 12 and 24 nM in the TR-FRET and SH-SY5Y assays, respectively.

To investigate whether the cellular potency and permeability profile could be further improved for this new structure class, we aimed to increase the lipophilicity and pK_a of the compounds. An increase in lipophilicity has been reported to increase the chance of a high permeability.^{22,48} As described above, we wanted to take advantage of the increased potency in the cellular assay by increasing pK_a of the compounds. Since the R^2 substituents are directly adjacent to the core, modifications to R^2 were predicted to give the largest impact on pK_a . Thus, R^2 substitution was varied with electron donating groups (Table 3). Adding a plain benzyl group, (*R*)-**1o** (isolated active enantiomer), increased the pK_a to 6.0. The potency in the TR-FRET assay decreased (e.g., compared to **1j**) probably because of the loss of the hydrogen bond interaction with Trp76. However, in the cellular assay (*R*)-**1o** gave increased potency, likely driven by the increase in pK_a . Four more analogues (**1p**–**1s**) with alkyl/heteroalkyl substituents in the R^2 -position were prepared and showed potencies in the low micromolar to high nanomolar range. Compounds **1r** and **1s** contain a hydrogen-bond acceptor moiety in R^2 , but the lack of potency

improvement points to an unoptimized interaction to Trp76 (Table 3). As seen with **1n**, by introduction of an $S3sp$ alkyne substituent in R^3 , the potency was increased more than 3-fold in both BACE-1 inhibition assays when going from **1p** (R^3 = 5-chloropyridin-3-yl, TR-FRET IC_{50} = 0.31 μ M) to **1t** (R^3 = 5-(prop-1-ynyl)pyridin-3-yl, TR-FRET IC_{50} = 0.079 μ M).

The highest LE of the reported compounds was seen for **1t** (R^2 = cyclopropyl, LE = 0.39). This can be compared to the analogue **1n** (R^2 = 3,5-dimethyl-4-methoxyphenyl, LE = 0.32). From the crystal structure of **1t** (only the *R*-enantiomer of the compound interacted with the protein to give a crystal structure) it became clear that the small cyclopropyl substituent (R^2) allowed the protein to maintain the intramolecular hydrogen bond between Trp76 and Tyr71, and the cyclopropyl is engaged in a hydrophobic interaction with Tyr71 (3.6 Å).²³ This should be compared to compounds with larger R^2 -substituents like (*S*)-**1m** (Figure 3).

In summary, the compounds with R^2 = alkyl/heteroalkyl had increased (about 1 log unit) pK_a values compared to the compounds with R^2 = aryl. The relative potency in the cellular assay compared to the TR-FRET assay increased, but for these compounds the overall potencies were lower presumably because of the loss of the hydrogen bond interaction to Trp76 (Figure 4). In addition, the hERG affinity increased for these more lipophilic compounds. The permeability profile for the compounds with R^2 = alkyl/heteroalkyl improved, with examples of low and medium efflux, e.g., (*R*)-**1o** and **1q**. A trend for these compounds was observed in which a low polar surface area (PSA) in combination with high ElogD values gave better permeability. In particular, the permeability for **1p** and **1q** was good.

To further increase the potency of compounds with alkyl/heteroalkyl as R^2 , we investigated the possibility of introducing a new interaction with the protein. From the crystal structures

Table 2. Aminoimidazoles **1a**–**n**, Measurements of BACE-1 Potency in TR-FRET Assay and SH-SY5Y Assay, Permeability Estimations ($P_{app}(A \rightarrow B)$ in Caco-2 Cells, Efflux Classifications from MDCK-MDR1 Cells), hERG, pK_a , ElogD, Solubility, PSA, and LE^a

compd	BACE-1 TR-FRET, ^b IC_{50} (μ M)	BACE-1 SH-SY5Y, ^b IC_{50} (μ M)	P_{app} (10^{-6} cm/s) ^c	efflux classification ^d	hERG, ^e IC_{50} (μ M)	pK_a ^f	ElogD ^g	solubility ^h (μ M)	PSA (\AA^2)	LE ⁱ
1a	not active	nd	46	nd	>33	5.4	2.1	199	57	
1b	>100	32	38	nd	>33	5.9	1.1	400	57	<0.25
1c	3.5	2.2	34	nd	16.7	6.5	2.2	157	56	0.34
1d	13	4.3	30	medium	>33	6.7	0.2	383	57	0.33
1e	18	nd	30	nd	>33	5.2	2.4	45	68	0.24
1f	2.1	2.8	30	nd	26.8	5.3	2.4	338	77	0.27
1g	1.3	1.9	nd	nd	nd	nd	1.8	63	57	0.32
1h	0.17	2.8	40	nd	nd	nd	nd	nd	67	0.34
1i	0.49	1.4	41	high	>33	4.9	2	35	57	0.33
1j	0.27	1.3	21	high	>33	5.2	1.1	358	77	0.33
1k	0.33	0.81	28	high	19	5.7	1.7	317	67	0.33
1l	0.097	0.17	19	high	>33	nd	1.7	255	77	0.34
1m	0.032	0.049	28	nd	>33	5.3	1.9	271	77	0.35
(<i>R</i>)- 1m	1.5	0.4	21	high	>33	nd	1.8	259	77	0.27
(<i>S</i>)- 1m	0.012	0.024	22	high	>33	5.2	1.8	258	77	0.37
1n	0.026	0.014	12	nd	17.5	nd	3.7	23	67	0.32

^and: not determined. ^b IC_{50} values are the mean of at least two experiments. ^c P_{app} is the measured permeability (A→B) through Caco-2 cells. ^dEfflux ratio is $P_{app}(B \rightarrow A)/P_{app}(A \rightarrow B)$ in MDCK-MDR1 cells. ^eMeasured in hERG-expressing CHO cells using IonWorks technology.⁴¹ ^fDetermined by pressure-assisted capillary electrophoresis.^{42,43} ^gDetermined by reversed phase liquid chromatography.⁴⁰ ^hDetermined by dried DMSO, a rapid throughput equilibrium solubility measurement.⁴⁴ ⁱLigand efficiency (LE)⁴⁵ calculated from TR-FRET data.

Table 3. Aminoimidazoles (*R*)-1o–t, measurements of BACE-1 Potency in TR-FRET Assay and SH-SY5Y Assay, Permeability Estimations ($P_{app}(A \rightarrow B)$ in Caco-2 Cells and Efflux Classifications from MDCK-MDR1 Cells), hERG, pK_a , ElogD, Solubility, PSA, and LE^a

compd	BACE-1 TR-FRET, ^b IC ₅₀ (μM)	BACE-1 SH-SY5Y, ^b IC ₅₀ (μM)	P_{app} (10 ⁻⁶ cm/s) ^c	efflux classification ^d	hERG, ^e IC ₅₀ (μM)	pK_a ^f	ElogD ^g	solubility ^h (μM)	PSA (Å ²)	LE ⁱ
(<i>R</i>)- 1o	2.6	0.71	31	low	>33	6.0	1.2	233	68	0.29
1p	0.31	0.69	57	high	12.4	nd	2	62	57	0.38
1q	1.4	0.66	41	medium	28.8	6.2	2.6	59	57	0.32
1r	3	4	22	high	21	6.0	2.5	272	65	0.28
1s	0.8	1.7	3	high	>33	5.7	2.1	257	76	0.28
1t	0.079	0.19	27	high	14.4	5.8	2.3	67	57	0.39

^and: not determined. ^bIC₅₀ values are the mean of at least two experiments. ^c P_{app} is the measured permeability (A→B) through Caco-2 cells. ^dEfflux ratio is $P_{app}(B \rightarrow A)/P_{app}(A \rightarrow B)$ in MDCK-MDR1 cells. ^eMeasured in hERG-expressing CHO cells using IonWorks technology.⁴¹ ^fDetermined by pressure-assisted capillary electrophoresis.^{42,43} ^gDetermined by reversed phase liquid chromatography.⁴⁰ ^hDetermined by dried DMSO, a rapid throughput equilibrium solubility measurement.⁴⁴ ⁱLigand efficiency (LE)⁴⁵ calculated from TR-FRET data.

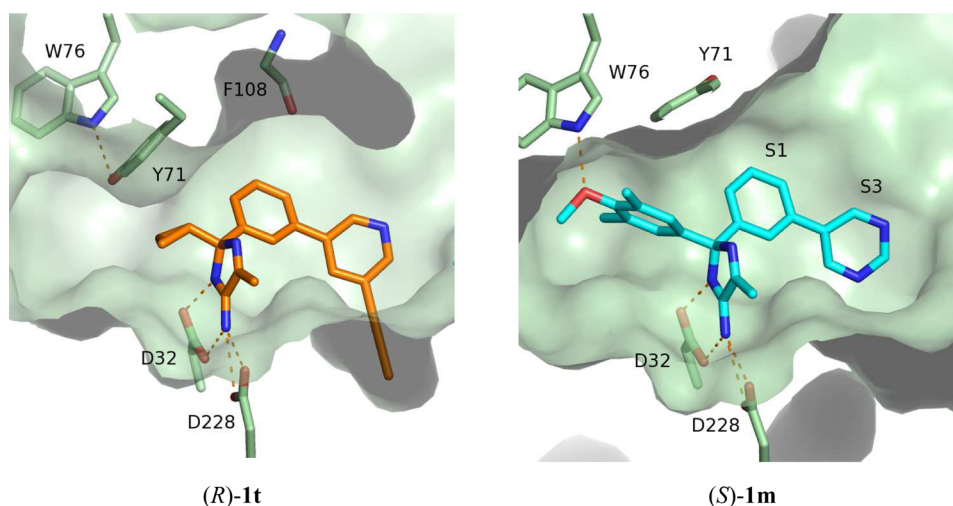


Figure 3. Crystal structure of (*R*)-**1t** (orange) and (*S*)-**1m** (cyan) complexed with BACE-1. For ligand (*R*)-**1t** with a small substituent, (R^2 = cyclopropyl) the internal hydrogen bond between Trp76 and Tyr71 was retained. Also shown is the interaction of Trp76 with the R^2 4-methoxy group for (*S*)-**1m**.

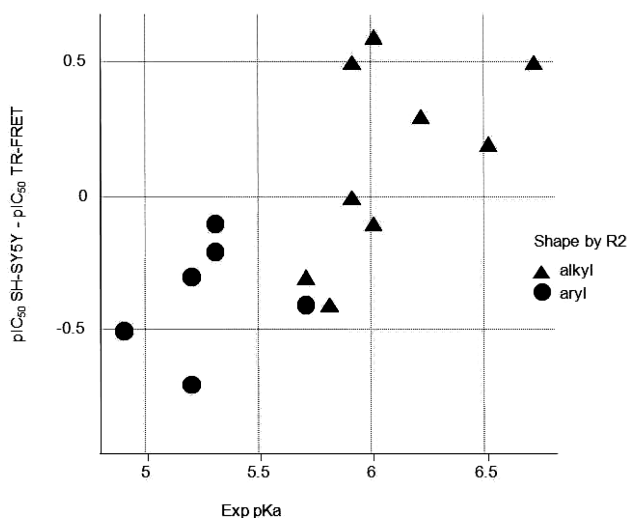


Figure 4. Correlation between potency change (pIC_{50} SH-SY5Y - pIC_{50} TR-FRET) and pK_a for the compounds **1a–v** (correlation factor $R^2 = 0.55$). R^2 -alkyl/heteroalkyl gives in general higher pK_a values than R^2 -aryl.

it seemed possible to establish a donor interaction between the S1 phenyl and the backbone carbonyl of Phe108 (Figure 3). Indeed, the introduction of a hydroxyl group to **1t** to give **1u** gave an additional 3-fold potency gain in the cellular assay compared to **1t** (Table 4). Unfortunately and possibly because of the extra hydrogen bond donor, the Caco-2 permeability decreased significantly.⁴⁸ The permeability $P_{app}(A \rightarrow B)$ in Caco-2 cells dropped from 27 for **1t** to 2.2 for **1u**, and the efflux ratio (in Caco-2 cells) increased from 0.8 for **1t** to 17 for **1u**.

In an effort to increase the permeability by tuning the hydrogen bond donor strength of the hydroxyl group, the position of the pyridine nitrogen in the biaryl moiety was shifted to allow for a possible intramolecular hydrogen bond (**1v**, Table 4).^{49,50} Indeed, permeability was improved for **1v** (Caco-2 cell data: $P_{app} = 19 \times 10^{-6}$ cm/s and efflux ratio is 0.5), but the potency for **1v** is approximately 2-fold lower than for **1u** possibly because the hydroxyl is no longer as available for hydrogen bonding to the protein.

Selectivity. Prior to further investigation, the selectivity toward cathepsin-D and BACE-2 was measured for a few compounds (Table 5). For cathepsin-D all compounds tested showed less than 30% inhibition at the highest concentration tested (100 μM). The BACE-2 activity showed higher variation, with 70-fold selectivity for (*S*)-**1m** but no selectivity for **1p** and

Table 4. Aminoimidazoles 1u and 1v, Measurements of BACE-1 Potency in TR-FRET Assay and SH-SY5Y Assay, Permeability Estimations ($P_{app}(A \rightarrow B)$) and Efflux Ratios in Caco-2 Cells), hERG, pK_a , ElogD, Solubility, PSA, and LE^a

compd	BACE-1 TR-FRET, ^b IC ₅₀ (μM)	BACE-1 SH-SY5Y, ^b IC ₅₀ (μM)	P_{app} (10 ⁻⁶ cm/s) ^c	efflux ratio ^d	hERG, ^e IC ₅₀ μM	pK_a ^f	ElogD ^g	solubility ^h (μM)	PSA (Å ²)	LE ⁱ
1u	0.061	0.058	2	17	24.5	5.9	1.2	400	80	0.38
1v	0.13	0.1	19	0.5	nd	nd	2.9	4	80	0.36

^and; not determined. ^bIC₅₀ values are the mean of at least two experiments. ^c P_{app} is the measured permeability (A→B) through Caco-2 cells. ^dEfflux ratio is $P_{app}(B \rightarrow A)/P_{app}(A \rightarrow B)$ in Caco-2 cells. ^eMeasured in hERG-expressing CHO cells using IonWorks technology. ^fDetermined by pressure-assisted capillary electrophoresis.^{42,43} ^gDetermined by reversed phase liquid chromatography.⁴⁰ ^hDetermined by dried DMSO, a rapid throughput equilibrium solubility measurement.⁴⁴ ⁱLigand efficiency (LE)⁴⁵ calculated from TR-FRET data.

Table 5. Amino-2H-imidazoles 1, Selectivity

compd	BACE-1 FRET, ^a IC ₅₀ (μM)	BACE-2 FRET, ^a IC ₅₀ (μM)	cath-D FRET, ^b % inhibition
(S)- 1m	0.012	0.84	30
1p	0.31	0.11	21
1t	0.079	0.030	8.5

^aIC₅₀ values are the mean of at least two experiments. ^b% inhibition at highest concentration tested (100 μM).

It. Selectivity data for more compounds will be needed in order to fully understand the selectivity profile for this new class of BACE-1 inhibitors.

Brain Exposure and in Vivo Efficacy Studies. To evaluate this core further and to understand the impact of the high efflux mentioned above, the brain exposure in mice was examined. Correction for blood content in brain was made by subtracting 1.3% of the plasma concentration from the total brain concentration. Free brain and plasma concentrations were calculated using brain and plasma protein binding data determined ex vivo. Compounds **1k**, (S)-**1m**, and **1t** had a low free brain/plasma ratio of 0.08, 0.05, and 0.07, respectively (Table 6). This was slightly improved with compound **1p** (0.16). However, **1p** had a lower potency in the TR-FRET and SH-SY5Y assays; therefore, compound (S)-**1m**, with a good overall profile, was selected for further in vivo studies.

As a consequence of the low exposure in mice, the pharmacodynamic effects of (S)-**1m** were studied in vivo in guinea pigs. Male guinea pigs ($n = 6$) received vehicle or (S)-**1m**, 50 or 100 μmol/kg, via oral gavage, and then plasma, cerebrospinal fluid (CSF), and brain samples were collected between 0.5 and 6 h after dose. Compound (S)-**1m** demonstrated a time- and dose-dependent reduction of Aβ in plasma, brain, and CSF (Figure 5, dose response data not shown). Maximum reductions of brain Aβ40 and Aβ42 (~50% and ~40%, respectively) were observed 1.5 h after dose, and the maximum plasma Aβ40 and Aβ42 diminutions (~70% and ~80%, respectively) were observed 3 h after dose. CSF Aβ40 displayed maximum effect 3 h after dose and was only

statistically significantly reduced, compared to vehicle, at this time point. This could be due to a larger individual variation of the basal levels of CSF Aβ and/or a delay in CSF effect versus brain. Six hours after dose the Aβ levels in brain and CSF were returning back to baseline, while plasma Aβ still was reduced (40–60%).

The exposure of (S)-**1m** was also measured in guinea pig plasma and brain samples to allow quantification of the PK/PD relationship for (S)-**1m**. The brain Aβ40 EC₂₀ for unbound compound (S)-**1m** was estimated (using brain tissue binding; see Experimental Section) to be 23 nM. Compound (S)-**1m** exhibited brain penetration with a ratio of 0.16 free exposure in brain versus the free exposure in plasma.

CONCLUSIONS

Amino-2H-imidazoles (**1**) represent a new class of BACE-1 inhibitors. The core structure differs from earlier reported cores regarding polarity, size, and pK_a of the amidine. In this report we present new synthetic methods toward diverse amino-2H-imidazoles, with three different methods used to prepare the 24 compounds for which data on primary activity, hERG activity, and permeability estimations are reported. These new compounds show good BACE-1 inhibition in both the enzymatic and cellular assays with nanomolar IC₅₀ values. By variation of the R²-substituent, it was possible to tune the pK_a of the compounds to effect an increase in potency in the cellular assay. In a matched pair analysis, one analogue with this new core showed an improved hERG profile compared to an earlier reported series. The permeability for this series was good, while the P-gp-mediated efflux was medium to high. Compound (S)-**1m** displayed an IC₅₀ of 24 nM in a cellular assay, and in an animal study this compound produced a concentration and time dependent decrease in Aβ40 and Aβ42 levels in plasma, brain, and CSF. Future research will elucidate the further potential of this series.

EXPERIMENTAL SECTION

BACE-1 TR-FRET Assay. The soluble part of human β-secretase (AA1-AA460) diluted in reaction buffer (sodium acetate, CHAPS, Triton X-100, EDTA, pH 4.5) was mixed with the test compound

Table 6. Mouse Plasma and Brain Exposure and Free Brain Plasma Ratio at 1.5 h after Intravenous (iv) or Oral (po) Dose^a

compd	dose, μmol/kg	dose route	time after dose, h	<i>n</i>	plasma concn, μmol/L	PPB, % free	free plasma concn, μmol/L	brain concn, μmol/L	brain binding, % free	free brain concn, nmol/L	free brain plasma ratio
1k	30	iv	1.5	3	11.5 ± 9.8	6.3	0.72 ± 0.62	0.71 ± 0.60	7.6	54 ± 45	0.08 ± 0.02
1p	30	iv	1.5	3	1.2 ± 0.4	4.6	0.06 ± 0.02	0.18 ± 0.08	4.8	9 ± 4	0.16 ± 0.02
1t	30	iv	1.5	3	3.7 ± 0.8	8.2	0.31 ± 0.06	0.98 ± 0.25	2.2	21 ± 6	0.07 ± 0.01
(S)- 1m	100	po	1.5	6	4.5 ± 1.9	11	0.49 ± 0.20	0.23 ± 0.06	8.2	19 ± 5	0.05 ± 0.02

^aMean ± SD.

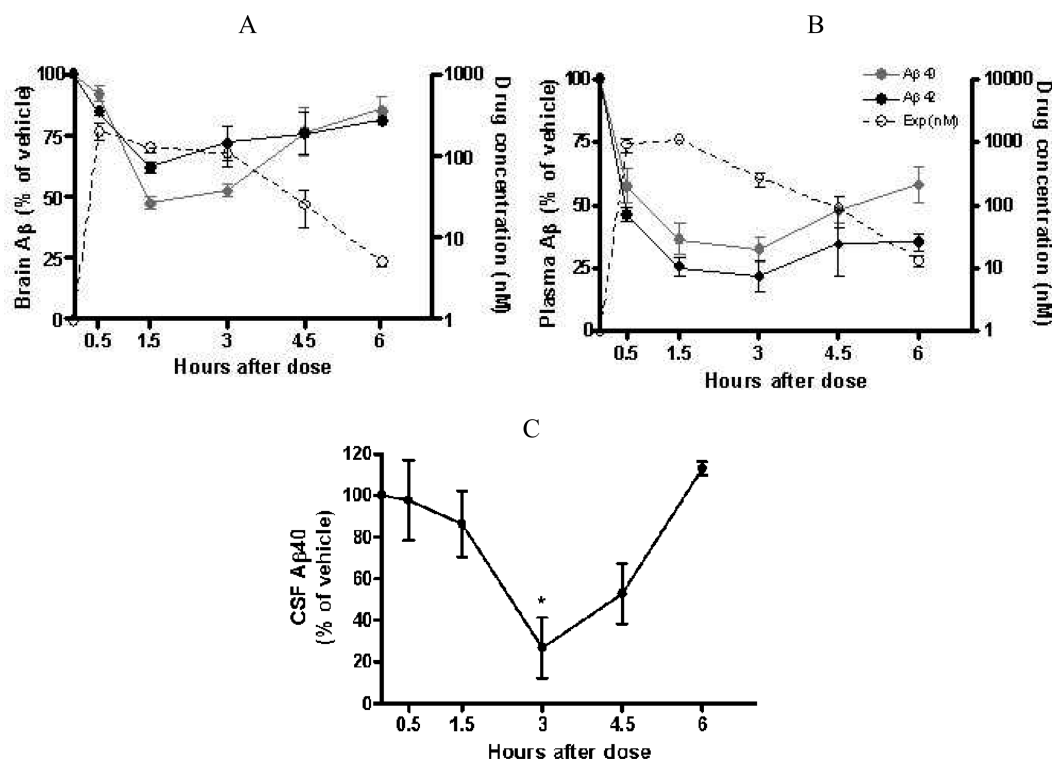


Figure 5. In vivo efficacy of (S)-1m. Time response effect on brain Aβ40/42 (A) and plasma Aβ40/42 (B) after an oral dose, 100 μmol/kg, of (S)-1m to male guinea pigs. The right y-axes show free compound exposure in brain and plasma (open circles and dotted line, respectively). Time response effects on CSF Aβ40 (C). CSF Aβ40 reached a statistical significant reduction compared to vehicle 3 h after an 100 μmol/kg dose (*, $P < 0.05$). Data shown are the mean and standard error of the mean (SEM) as % of vehicle Aβ levels.

diluted in DMSO. After a preincubation period of 10 min, substrate (europium)CEVNLDAEFK(Qsy7) was added and the reaction allowed to proceed for 15 min at room temperature. The reaction was stopped by addition of 7 μL of sodium acetate, pH 9. The fluorescence of the product was measured on a Victor II plate reader with an excitation wavelength of 340 nm and an emission wavelength of 615 nm. The final concentration of the enzyme was 2.7 μg/mL. The final concentration of substrate was 100 nM. Reported values are the mean of $n \geq 2$ determinations, with standard deviation up to 10%.

Cell sAPPβ Release Assay. SH-SY5Y cells (human neuroblastoma cell line) were cultured in DMEM/F-12 with Glutamax, 10% FCS, and 1% nonessential amino acids (Invitrogen). The test compound was incubated with cells for 16 h at 37 °C, 5% CO₂. Meso Scale Discovery (MSD) plates were used for the detection of sAPPβ release according to the manufacturer's instructions, and the plates were read in a SECTOR Imager. In addition, the cells incubated with test compound were further lyophilized and analyzed for any cytotoxic effects of the compounds using the ViaLight Plus cell proliferation/cytotoxicity kit (Cambrex BioScience) according to the manufacturer's instructions. Reported values are the mean of $n \geq 2$ determinations, with standard deviation up to 10%.

BACE-2 TR-FRET Assay. This assay is as described for the BACE-1 TR-FRET assay above but utilizing the soluble part of human β-secretase 2 enzyme (AA1-AA473).

hCathepsin-D FRET Assay. Cathepsin-D enzyme (Calbiochem) and substrate (Ac-Glu-Asp(EDANS)-Lys-Pro-Ile-Leu-Phe-Phe-Arg-Leu-Gly-Lys(DABCYL)-Glu-NH₂) (Bachem) were separately diluted in glycine-HCl buffer. The cathepsin-D solution was mixed with compound in DMSO and preincubated for 10 min. The substrate solution was added, and the reaction mixture was incubated for 15 min in darkness at 22 °C. The fluorescent signal was measured in a Wallac 1420 multilabel counter Victor2 at 355 nm excitation and 460 nm emission.

Protein Crystallography. The human BACE-1, CID1328 14-453, was cloned, expressed, refolded, activated, and purified according to

previously published protocols.⁵¹ The protein buffer was exchanged to 20 mM Tris, pH 8.5, 150 mM NaCl and concentrated to 3.5 mg/mL. Concentrated protein was mixed 1:1 with a stock of 11% PEG6k and 100 mM sodium acetate, pH 5.0, at room temperature and crystallized using vapor diffusion techniques in combination with seeding. The crystals were soaked with 10 mM (S)-1m and 1t, respectively, 10% DMSO, 18% PEG6000, 90 mM sodium acetate, pH 4.85, 18 mM Tris, pH 8.5, and 135 mM NaCl for 24 h and flash frozen in liquid nitrogen using 20% glycerol as a cryoprotectant.

Data of (S)-1m and 1t soaked crystals were collected on a Rigaku FR-E+ SuperBright rotating anode and a HTC imaging plate to 1.95 Å resolution. All data were indexed and integrated with MOSFLM⁵² and scaled with SCALA⁵³ in space group P212121, with cell dimensions of about [48, 76, 105 Å], giving a Matthews coefficient of 2.2 Å³/Da with one monomer per asymmetric unit. The (S)-1m and 1t structures were solved by rigid body refinement of a previously determined BACE-1 structure based on the published 1FKN structure⁵⁴ using Refmac5.⁵⁵ The initial models were further refined by alternative cycles of model rebuilding in Coot⁵⁶ and refinement in Refmac5 and AutoBuster.⁵⁷ The (S)-1m and 1t compounds were placed in the refined omit maps by Flynn.⁵⁸ Final refinement of the BACE-1 inhibitor complexes was performed in Refmac5 and AutoBuster. Resulting 2F_o - F_c maps of the compounds (S)-1m and (R)-1t can be seen in Supporting Information Figures 1 and 2. Full data collection and refinement statistics can be found in Supporting Information Table 1.

Permeability Assays. Caco-2 cells were grown for 14–21 days to achieve confluency and polarization before being used for transport experiments. For both apical to basolateral (A–B) and basolateral to apical (B–A) transport directions, the pH was adjusted to 7.4. All compounds were investigated at 10 μM. Buffer volumes in the 42-well plates were 0.20 mL on the apical side and 0.80 mL on the basolateral side. Samples were withdrawn after 30 or 60 min. The integrity of the epithelial cell monolayer was monitored by measuring the passive transmembrane diffusion of [¹⁴C]mannitol. Concentrations of

compounds in donor and receiver samples were analyzed by liquid chromatography–tandem mass spectrometry. Liquid scintillation was used for analysis of [^{14}C]mannitol. The apparent permeability coefficient P_{app} was calculated according to $P_{\text{app}} = (dQ/dt)/(AC_0)$, where dQ/dt is the slope at 30 or 60 min of the graph of the cumulative amount transported vs time, A is the surface area of the membrane, and C_0 is the starting concentration. The efflux ratio is the ratio $P_{\text{app}}(\text{B}-\text{A})/P_{\text{app}}(\text{A}-\text{B})$.

MDCK-MDR1 efflux data were generated using a Transwell assay as described by Ledonne et al.⁵⁹ with minor adaptations. Cells were sown at 400 000–600 000 cells per well in a 96-well plate and cultured for 3–5 days. Testing was at 1 μM compound concentration, and the efflux incubation time was 2.5 h. This was shortened to 60 min when the compound concentration was 10 μM . In each format the compounds were classified as low (efflux ratio of <2.5), medium (efflux ratio between 2.5 and 3.5), or high (efflux ratio of >3.5) efflux.

Plasma Protein and Brain Tissue Binding. Compounds were added to mouse or guinea pig plasma to a final concentration of 10 μM . An aliquot of 180 μL was transferred to a dialysis plate with phosphate buffer on the other site and incubated for 18 h at 37 $^{\circ}\text{C}$. Proteins were removed from aliquots (50 μL) of plasma and buffer samples. The internal standard was added, and the samples were analyzed with LC–MS/MS. The unbound fraction in plasma was calculated from the ratio of the MS area of compound in buffer divided by sum of the areas of compound in buffer and plasma. Recovery and stability in plasma were controlled.

To determine brain tissue binding, 300 μm thick coronal rat brain slices were incubated for 5 h in 10 mL of an artificial interstitial fluid buffer containing 1 μM compound. Following the incubation, slices were weighted and homogenized, proteins were removed, and LC–MS/MS analysis was performed. The unbound fraction in brain was calculated as described earlier.⁶⁰ Mouse and guinea pig total brain concentrations were converted to free concentrations by multiplying with the unbound fraction.

Animals and Animal Handling. All animal experimentations were performed in accordance with relevant guidelines and regulations provided by the Swedish Board of Agriculture. The ethical permissions were provided by an ethical board specializing in animal experimentations, the Stockholm Norra Animal Research Ethical Board.

Mice Exposure Studies. To study brain exposure, female C57BL/6 mice purchased from Harlan Laboratories, The Netherlands, were sacrificed 1.5 h after an intravenous (iv) dose with 30 $\mu\text{mol}/\text{kg}$ **1k** in 0.1 M gluconic acid or with 30 $\mu\text{mol}/\text{kg}$ **1p** in 5% dimethylacetamide and 0.1 M meglumine or with 30 $\mu\text{mol}/\text{kg}$ **1t** in 5% dimethylacetamide and 0.1 M gluconic acid, 3 mice per compound. Six female C57BL/6 mice were dosed by oral gavage (po) with 100 $\mu\text{mol}/\text{kg}$ (S)-**1m** in 5% dimethylacetamide, 20% hydroxypropyl β -cyclodextrin in 0.3 M gluconic acid, pH 4, and sacrificed 1.5 h after dose. Animals were anesthetized before plasma and brain samples were collected. Plasma was isolated from blood collected by cardiac puncture into EDTA tubes and was centrifuged for 10 min at approximately 3000g at 4 $^{\circ}\text{C}$ within 20 min of sampling. Animals were then sacrificed by decapitation to collect brains.

In Vivo Pharmacokinetic Assay. Brain and plasma exposure and plasma protein and brain tissue binding were performed as previously described.⁶¹ Briefly, right brain hemispheres of guinea pig or whole brains of mice were homogenized in 2 volumes (w/v) of Ringer solution. Aliquots of plasma (25 μL) and brain homogenate (50 μL) were precipitated with 150 μL of acetonitrile containing a generic internal standard (200 nmol/L warfarin). Samples were mixed, centrifuged, appropriately diluted with mobile phase, and analyzed on a LC–MS/MS system. Brain exposure was corrected for compound exposure in plasma/blood present in the brain sample, since no brain perfusion was performed, by assuming 1.3% blood/plasma in brain.

In Vivo Efficacy Assay. Male 5- to 11-week-old Dunkin–Hartley (DH) guinea pigs purchased from HB Lidköping Kaninfarm (Lidköping, Sweden) were used. The guinea pigs (six in each experimental group) received vehicle or compound (S)-**1m** at 50 or

100 $\mu\text{mol}/\text{kg}$ via oral gavage. As vehicle, 20% HP β CD in 0.3 M gluconic acid (pH 5) were used.

Animals were anesthetized 0.5, 1.5, 3, 4.5, or 6 h after administration of vehicle or drug and were then kept under isoflurane anesthesia during the rest of the procedures. Cerebrospinal fluid (CSF) was aspirated from the cisterna magna, and plasma was isolated from blood collected by cardiac puncture into EDTA tubes. All samples were centrifuged for 10 min at approximately 3000g at 4 $^{\circ}\text{C}$ within 20 min of sampling to remove cells or debris. Animals were then sacrificed by decapitation, and brains were dissected into hemispheres.

The left brain hemispheres from the guinea pigs were homogenized in 0.2% diethylamine (DEA) with 50 mM NaCl, followed by ultracentrifugation. Recovered supernatants were neutralized to pH 8.0 with 2 M Tris-HCl. Prior to analysis the buffer was exchanged to sample diluents enclosed in commercial ELISA kits. In addition samples for A β 40 analysis were concentrated 2 times and samples for A β 42 analysis diluted 2 times. A β 40 and A β 42 levels in brain extracts, CSF, and plasma were analyzed using commercial A β 1–40 (no. KMB3481, Invitrogen, Camarillo, CA) and A β 1–42 (80177 RUO, Innogenetics, Gent, Belgium) ELISA kits.

Analysis of A β data was performed using Prism 4 (GraphPad, U.S.), with one-way ANOVA followed by Dunnett's multiple comparison test or Bonferroni's multiple comparison test. Level of significance was set at $P < 0.05$.

Pharmacokinetic/Pharmacodynamic Analysis of in Vivo Exposure and Effect Data in Guinea Pig. The relationship between plasma exposure and brain A β 40 effect data was analyzed by fitting the plasma PK profile and letting the fitted plasma profile drive the PD effect using Pharsight WinNonlin 5.2 software. A reparametrized indirect response model with inhibition on the production rate⁶² was used to estimate the plasma concentration, giving 20% inhibition from baseline (IC₂₀). This plasma EC₂₀ was converted to free brain concentration using plasma protein and brain binding and brain exposure data.

Chemistry. All solvents used were commercially available and were used without further purification. Reactions were typically run using anhydrous solvents under an inert atmosphere of nitrogen or argon. Starting materials used were available from commercial sources or prepared as described in Supporting Information. Room temperature refers to 20–25 $^{\circ}\text{C}$. Microwave heating was performed in a Biotage Initiator microwave synthesizer at the indicated temperature in the recommended microwave tubes.

^1H NMR spectra were recorded in the indicated deuterated solvent at 400 MHz, and the spectra were obtained unless stated otherwise, using a Bruker av400 NMR spectrometer equipped with a 3 mm flow injection SEI $^1\text{H}/\text{D}-^{13}\text{C}$ probe head with Z-gradients, using a BEST 215 liquid handler for sample injection or using a Bruker DPX400 NMR spectrometer equipped with a four-nucleus probe head (^{19}F) with Z-gradients. 500 MHz spectra were recorded using a Bruker 500 MHz Avance III NMR spectrometer. Chemical shifts are given in ppm downfield and upfield from TMS. Resonance multiplicities are denoted s, d, t, q, m, and br for singlet, doublet, triplet, quartet, multiplet, and broad, respectively.

Preparative HPLC was performed on a Waters Auto purification HPLC–UV system with a diode array detector using a Waters XTerra MS C₈ column (19 mm \times 300 mm, 7 μm), and a linear gradient of mobile phase B was applied. Mobile phase A was 0.1 M ammonium acetate in water/acetonitrile (95:5), and mobile phase B was acetonitrile. Flow rate was 20 mL/min. Flash chromatography was performed using Merck silica gel 60 (0.040–0.063 mm) or employing a Combi Flash Companion system using RediSep normal-phase flash columns.

Column chromatography was performed using Merck silica gel 60 (0.040–0.063 mm).

LC–MS analyses were performed on an LC–MS instrument consisting of a Waters sample manager 2777C, a Waters 1525 μ binary pump, a Waters 1500 column oven, a Waters ZQ single quadrupole mass spectrometer, a Waters PDA 2996 diode array detector, and a Sedex 85 ELS detector. The mass spectrometer was equipped with an electrospray ion source (ES) operated in positive and negative ion

modes. For separation a linear gradient was applied starting at 100% 0.1% NH₃ in Milli-Q ending at 100% methanol. The column used was an XBridge C18, 3.0 mm × 50 mm, 5 μm, which was run at a flow rate of 2 mL/min. Or an LC-MS system was used consisting of a Waters Alliance 2795 HPLC, a Waters PDA 2996 diode array detector, a Sedex 85 ELS detector, and a ZQ single quadrupole mass spectrometer. The mass spectrometer was equipped with an electrospray ion source (ES) operated in positive and negative ion modes. Separation was performed on an XBridge C18, 3.0 mm × 50 mm, 3.5 μm, at a flow rate of 1 mL/min. A linear gradient was applied starting at 100% 0.1% NH₃ in Milli-Q and ending at 100% methanol.

Purity analyses were performed on an Agilent HP1100 system consisting of a G1322A microvacuum degasser, a G1312A binary pump, a G1367A well-plate autosampler, a G1316A thermostated column compartment, a G1315C diode array detector, and a 6120, G1978B mass spectrometer. The mass spectrometer was configured with an atmospheric pressure chemical ionization (APCI) ion source operated in positive and negative ion modes. The column used was an XBridge C18 3.0 mm × 100 mm, 3 μm run at a flow rate of 1.0 mL/min. A linear gradient was used for both the blank and the sample, starting at 100% 10 mM NH₄OAc in 5% CH₃CN and ending at 95% CH₃CN. The blank run was subtracted from the sample run. All tested compounds were purified to >95% purity as determined by reversed phase HPLC.

SFC purity analysis was run on a SFC Berger Analytix system with Agilent 1100 PDA detector. The column was a Chiralpak AD-H, 5 μm, 4.6 mm × 250 mm. The column temperature was set to 50 °C. An isocratic condition of 20–30% methanol + 0.1% DEA and 70–80% CO₂ was applied at a flow rate of 3.0 mL/min. The PDA was set to scan from 190 to 600 nm, and the data at 220 nm were extracted for purity determination. All tested compounds were purified to >99% enantiomeric purity as determined by SFC.

SFC preparative chromatography was run on a SFC Berger Multigram II system with a Knauer K-2501 UV detector. The column was a Chiralpak AD-H, 5 μm, 21.2 mm × 250 mm. The column temperature was set to 35 °C. An isocratic condition of 20–30% methanol + 0.1% DEA and 70–80% CO₂ was applied at a flow rate of 50.0 mL/min. The UV detector was set to scan at 220 nm. The UV signal determined the fraction collection.

2-Methyl-5-phenyl-2-(3-(pyridin-3-yl)phenyl)-2H-imidazol-4-amine (1a). *N*-Allyl-2-(3-bromophenyl)-2-methyl-5-phenyl-2H-imidazol-4-amine (**11**) (31 mg, 80 μmol), pyridin-3-ylboronic acid (16 mg, 0.13 mmol), and bis(triphenylphosphine)palladium(II) chloride (4 mg, 6 μmol) were taken up in DME (0.5 mL) and water (0.25 mL). Sodium carbonate (1 M) (0.21 mL, 0.21 mmol) was added, and the mixture was heated at 80 °C for 2.5 h. Pyridin-3-ylboronic acid (12 mg) and bis(triphenylphosphine)palladium(II) chloride (3 mg) were added, and the mixture continued heating for 2 h. The reaction mixture was evaporated and the residue treated with water and extracted with chloroform (3 × 3 mL). The dried (Na₂SO₄) organic phases were combined and evaporated in vacuo. To the product (30 mg) were added 1,3-dimethylbarbituric acid (77 mg, 0.49 mmol), tetrakis(triphenylphosphine)palladium(0) (9 mg, 8 μmol), and dichloromethane (0.8 mL) under argon, and the resulting mixture was subjected to microwave irradiation at 100 °C for 30 min. More 1,3-dimethylbarbituric acid (30 mg) and tetrakis(triphenylphosphine)palladium(0) (9 mg, 8 μmol) were added, and the mixture was subjected to microwave irradiation at 100 °C for another 30 min. The evaporated residue was dissolved in methanol and filtered. Reversed phase preparative-HPLC gave 7 mg (28%, over two steps) of the title compound. ¹H NMR (500 MHz, acetonitrile-*d*₃) δ ppm 8.85 (d, *J* = 1.9 Hz, 1 H), 8.56 (dd, *J* = 5.0, 1.6 Hz, 1 H), 7.96–8.01 (m, 1 H), 7.91 (t, *J* = 1.6 Hz, 1 H), 7.74–7.80 (m, 2 H), 7.68 (ddd, *J* = 7.7, 1.6, 1.4 Hz, 1 H), 7.50–7.59 (m, 4 H), 7.46 (t, *J* = 7.7 Hz, 1 H), 7.42 (dd, *J* = 7.6, 4.4 Hz, 1 H), 1.74 (s, 3 H); MS (ES+) *m/z* 327 [M + H]⁺.

5-Isopropyl-2-methyl-2-(3-(pyridin-3-yl)phenyl)-2H-imidazol-4-amine (1b). 2-(3-Bromophenyl)-5-isopropyl-2-methyl-2H-imidazol-4-amine (**7b**) (25 mg, 80 μmol), pyridin-3-ylboronic acid (26 mg, 0.2 mmol), and bis(triphenylphosphine)palladium(II) chloride (12 mg, 20 μmol) were taken up in DME (2 mL) and water (1 mL).

Sodium carbonate (1 M in water) (0.2 mL, 0.2 mmol) was added, and the mixture was heated at 80 °C for 2 h. Reversed phase preparative-HPLC gave 24 mg (81%) of the title compound. ¹H NMR (400 MHz, chloroform-*d*₃) δ ppm 1.33 (dd, *J* = 12.1, 6.8 Hz, 6 H), 1.76 (s, 3 H), 2.83 (dt, *J* = 13.6, 6.8 Hz, 1 H), 7.37 (dd, *J* = 7.6, 4.8 Hz, 1 H), 7.40–7.52 (m, 2 H), 7.62 (d, *J* = 7.6 Hz, 1 H), 7.81 (s, 1 H), 7.92 (dt, *J* = 7.9, 2.0 Hz, 1 H), 8.59 (dd, *J* = 4.8, 1.3 Hz, 1 H), 8.86 (d, *J* = 1.8 Hz, 1 H); MS (ES+) *m/z* 293 [M + H]⁺.

2-(3'-Methoxybiphenyl-3-yl)-2,5-dimethyl-2H-imidazol-4-amine (1c). 2-(3-Bromophenyl)-2,5-dimethyl-2H-imidazol-4-ol (**6c**) (76 mg, 0.28 mmol) was dissolved in pyridine (1.5 mL), and phosphorus pentasulfide (76 mg, 0.17 mmol) was added. The mixture was heated at 120 °C for 1 h. Ammonia (7 M in methanol) (4 mL, 28 mmol) and *tert*-butyl hydroperoxide (0.586 mL, 4.27 mmol) were added, and the mixture was stirred at room temperature for 16 h. The solvents were evaporated, and reversed phase preparative-HPLC gave 41 mg of the intermediate cyclic thioamide. The purified material, 3-methoxyphenylboronic acid (28 mg, 0.19 mmol), and bis(triphenylphosphine)palladium(II) chloride (11 mg, 20 μmol) were taken up in DME (2 mL) and water (1 mL). Sodium carbonate (1 M in water) (0.4 mL, 0.4 mmol) was added, and the mixture was heated at 80 °C for 2 h. Reversed phase preparative-HPLC gave 21 mg (26%, over two steps) of the title compound. ¹H NMR (400 MHz, chloroform-*d*₃) δ ppm 7.85 (t, *J* = 1.64 Hz, 1 H), 7.58–7.64 (m, *J* = 7.58, 1.26, 0.88, 0.88 Hz, 1 H), 7.46–7.51 (m, *J* = 7.74, 1.26, 0.93, 0.93 Hz, 1 H), 7.40 (t, *J* = 7.71 Hz, 1 H), 7.35 (t, *J* = 7.96 Hz, 1 H), 7.20 (ddd, *J* = 7.64, 1.58, 0.88 Hz, 1 H), 7.15 (dd, *J* = 2.53, 1.77 Hz, 1 H), 6.89 (ddd, *J* = 1.5, 2.59, 0.88 Hz, 1 H), 3.87 (s, 3 H), 2.29 (s, 3 H), 1.74 (s, 3 H); MS (ES+) *m/z* 294 [M + H]⁺.

2,5-Dimethyl-2-(3-(pyridin-3-yl)phenyl)-2H-imidazol-4-amine (1d). 2-(3-Bromophenyl)-2,5-dimethyl-2H-imidazol-4-ol (**6c**) (0.14 g, 0.52 mmol) was dissolved in pyridine (1.5 mL), and phosphorus pentasulfide (0.14 g, 0.31 mmol) was added. The mixture was heated at 120 °C for 1 h. Ammonia (7 M in methanol) (4 mL, 28 mmol) and *tert*-butyl hydroperoxide (1.1 mL, 7.8 mmol) were added, and the mixture was stirred at room temperature for 16 h. The solvents were evaporated, and reversed phase preparative-HPLC gave 95 mg of the intermediate cyclic thioamide. A portion of the purified material (40 mg), pyridin-3-ylboronic acid (37 mg, 0.30 mmol), and bis(triphenylphosphine)palladium(II) chloride (11 mg, 20 μmol) was taken up in DME (1 mL) and water (0.5 mL). Sodium carbonate (1 M in water) (0.376 mL, 0.38 mmol) was added, and the mixture was heated at 80 °C for 2 h. Reversed phase preparative-HPLC gave 30 mg (22%, over two steps) of the title compound. ¹H NMR (400 MHz, chloroform-*d*₃) δ ppm 8.85 (d, *J* = 1.52 Hz, 1 H), 8.58 (d, *J* = 3.79 Hz, 1 H), 7.92 (dd, *J* = 6.06, 2.02 Hz, 1 H), 7.81 (s, 1 H), 7.63 (d, *J* = 7.33 Hz, 1 H), 7.47 (dt, *J* = 15.41, 7.71 Hz, 2 H), 7.37 (dd, *J* = 7.83, 4.80 Hz, 1 H), 2.32 (s, 3 H), 1.76 (s, 3 H); MS (ES+) *m/z* 265 [M + H]⁺.

5-Isopropyl-2-phenyl-2-(3-(pyrimidin-5-yl)phenyl)-2H-imidazol-4-amine (1e). (3-Bromophenyl)(phenyl)methanone (0.23 g, 0.86 mmol) was dissolved in ammonia (7 M in methanol) (4 mL, 28 mmol), and the mixture was heated at 150 °C for 1 h by microwave irradiation. Ethyl 3-methyl-2-oxobutylate (1 mL, 6.9 mmol) was added in four portions (4 × 250 μL), and the mixture was stirred at 150 °C after each addition. The solvent was evaporated, and silica column chromatography (0:1 → 3:10, EtOAc/heptane) gave 49 mg of the cyclic amide. The purified material was dissolved in pyridine (1.5 mL), and phosphorus pentasulfide (50 mg, 0.11 mmol) was added. The mixture was heated at 120 °C for 1 h. Methanol (3 mL), ammonia (35% in water) (1 mL, 18 mmol), and *tert*-butyl hydroperoxide (0.28 mL, 2 mmol) were added, and the mixture was stirred at room temperature for 16 h. The solvents were evaporated, and reversed phase preparative-HPLC gave 16 mg of the intermediate aminoimidazole. The purified material, pyrimidin-5-ylboronic acid (11 mg, 90 μmol), and bis(triphenylphosphine)palladium(II) chloride (6 mg, 9 μmol) were taken up in DME (1 mL) and water (0.5 mL). Sodium carbonate (1 M in water) (0.11 mL, 0.11 mmol) was added, and the mixture was heated at 80 °C for 2 h. Reversed phase preparative-HPLC gave 13 mg (4%, over three steps) of the title compound. ¹H

NMR (400 MHz, chloroform- d_3) δ ppm 9.19 (s, 1 H), 8.93 (s, 2 H), 7.79 (s, 1 H), 7.67 (td, $J = 4.48, 1.64$ Hz, 1 H), 7.53–7.59 (m, 2 H), 7.43–7.47 (m, 2 H), 7.21–7.33 (m, 3 H), 5.30 (br s, 2 H), 2.82 (dt, $J = 13.64, 6.82$ Hz, 1 H), 1.37 (d, 6 H); MS (ES+) m/z 356 [M + H]⁺.

5-Isopropyl-2-(4-methoxyphenyl)-2-(3-(pyrimidin-5-yl)phenyl)-2H-imidazol-4-amine (1f). (3-Bromophenyl)(4-methoxyphenyl)methanone (0.4 g, 1.4 mmol) was dissolved in ammonia (7 M in methanol) (3.9 mL, 27 mmol), and ethyl 3-methyl-2-oxobutylate (1 mL, 6.9 mmol) was added in five portions (5 × 200 μ L). The mixture was stirred at 150 °C for 1 h with microwave irradiation after each addition. The solvent was evaporated, and reversed phase preparative-HPLC followed by silica column chromatography (0:1 → 1:0, EtOAc/heptane) gave 7 mg of the intermediate cyclic amide. The purified material was dissolved in pyridine (1 mL), and phosphorus pentasulfide (50 mg, 0.11 mmol) was added. The mixture was heated at 120 °C for 1 h. Ammonia (33% in water) (0.25 mL, 4.26 mmol) and *tert*-butyl hydroperoxide (0.3 mL, 2.18 mmol) were added, and the mixture was stirred at room temperature for 16 h. The solvents were evaporated, and reversed phase preparative-HPLC gave 6 mg of the intermediate aminoimidazole. The purified material, pyrimidin-5-ylboronic acid (4 mg, 30 μ mol), and bis(triphenylphosphine)palladium(II) chloride (2 mg, 3 μ mol) were taken up in DME (1 mL) and water (0.5 mL). Sodium carbonate (1 M in water) (40 μ L, 4 μ mol) was added, and the mixture was heated at 80 °C for 2 h. Reversed phase preparative-HPLC gave 5 mg (1%, over three steps) of the title compound. ¹H NMR (400 MHz, chloroform- d_3) δ ppm 9.19 (s, 1 H), 8.92 (s, 2 H), 7.76 (s, 1 H), 7.61–7.68 (m, 1 H), 7.48 (d, $J = 8.84$ Hz, 2 H), 7.41–7.45 (m, 2 H), 6.83 (d, $J = 8.84$ Hz, 2 H), 3.78 (s, 3 H), 2.81 (dt, $J = 13.64, 6.82$ Hz, 1 H), 1.36 (d, $J = 6.82$ Hz, 6 H); MS (ES+) m/z 386 [M + H]⁺.

5-Methyl-2-phenyl-2-(3-(pyridin-3-yl)phenyl)-2H-imidazol-4-amine (1g). (3-Bromophenyl)(phenyl)methanone (0.28 g, 1.1 mmol) was dissolved in ammonia (7 M in methanol) (4 mL, 28 mmol) and heated at 150 °C for 1 h with microwave irradiation. Ethyl 2-oxopropanoate (1 mL, 9 mmol) was added in five portions (5 × 200 μ L), and the mixture was stirred at 150 °C for 1 h with microwave irradiation after each addition. The solvent was evaporated, and reversed phase preparative-HPLC gave 11 mg of the cyclic amide. The purified material was dissolved in pyridine (1 mL), and phosphorus pentasulfide (50 mg, 0.11 mmol) was added. The mixture was heated at 120 °C for 1 h. Ammonia (7 M in methanol) (1 mL, 7 mmol) and *tert*-butyl hydroperoxide (0.5 mL, 3.6 mmol) were added, and the mixture was stirred at room temperature for 16 h. The solvents were evaporated, and reversed phase preparative-HPLC gave 8 mg of the intermediate aminoimidazole. The purified material, pyridin-3-ylboronic acid (6 mg, 50 μ mol), and bis(triphenylphosphine)palladium(II) chloride (3 mg, 5 μ mol) were taken up in DME (1 mL) and water (0.5 mL). Sodium carbonate (1 M in water) (57 μ L, 60 μ mol) was added, and the mixture was heated at 80 °C for 2 h. Reversed phase preparative-HPLC gave 2 mg (0.4%, over three steps) of the title compound. ¹H NMR (400 MHz, chloroform- d_3) δ ppm 8.82 (br s, 1 H), 8.57 (d, $J = 3.79$ Hz, 1 H), 7.86 (dt, $J = 7.83, 1.89$ Hz, 1 H), 7.81 (s, 1 H), 7.57–7.65 (m, 3 H), 7.37–7.47 (m, 2 H), 7.21–7.36 (m, 4 H), 2.36 (s, 3 H); MS (ES+) m/z 327 [M + H]⁺.

2-(3'-Methoxybiphenyl-3-yl)-5-methyl-2-(pyridin-4-yl)-2H-imidazol-4-amine (1h). (3-Bromophenyl)(pyridin-4-yl)methanimine (4h) (0.47 g, 1.8 mmol) was dissolved in ammonia (7 M in methanol) (3 mL, 21 mmol). Ethyl 2-oxopropanoate (1 mL, 9 mmol) was added in five portions (5 × 200 μ L), and the mixture was stirred at 150 °C for 1 h after each addition. Reversed phase preparative-HPLC gave 22 mg of the intermediate cyclic amide. The purified material was dissolved in pyridine (1 mL), and phosphorus pentasulfide (50 mg, 0.11 mmol) was added. The mixture was heated at 120 °C for 1 h. Ammonia (35% in water) (0.16 mL, 2.7 mmol) and *tert*-butyl hydroperoxide (0.14 mL, 1.0 mmol) were added, and the mixture was stirred at room temperature for 16 h. The solvents were evaporated, and reversed phase preparative-HPLC gave 4 mg of the intermediate aminoimidazole. The purified material, 3-methoxyphenylboronic acid (4 mg, 20 μ mol), and bis(triphenylphosphine)palladium(II) chloride (2 mg, 2 μ mol) were taken up in DME (1 mL)

and water (0.5 mL). Sodium carbonate (1 M in water) (30 μ L, 30 μ mol) was added, and the mixture was heated at 80 °C for 2 h. Reversed phase preparative-HPLC gave 1 mg (0.2%, over three steps) of the title compound. ¹H NMR (400 MHz, chloroform- d_3) δ ppm 8.54 (br s, 2 H) 7.80 (s, 1 H), 7.46–7.61 (m, 4 H), 7.31–7.43 (m, 2 H), 7.15 (d, $J = 7.83$ Hz, 1 H), 7.07–7.13 (m, 1 H), 6.89 (dd, $J = 8.34, 2.02$ Hz, 1 H), 3.86 (s, 3 H), 2.40 (s, 3 H); MS (ES+) m/z 357 [M + H]⁺.

2-(4-Fluorophenyl)-5-methyl-2-(3-(pyridin-3-yl)phenyl)-2H-imidazol-4-amine (1i). (3-Bromophenyl)(4-fluorophenyl)methanimine (4i) (1.0 g, 3.6 mmol) and ethanebis(thioamide) (0.58 g, 4.8 mmol) were taken up in methanol (5 mL). The mixture was heated at 90 °C for 3 days. The solvent was evaporated and the residue was purified by silica column chromatography (0:1 → 1:1, EtOAc/heptane) and reversed phase preparative-HPLC to give 0.15 g of the intermediate imidazolthiol. The purified material was dissolved in THF (5 mL). Iodomethane (0.075 mL, 1.2 mmol) was added, and the mixture was heated at reflux for 8 h. The reaction mixture was filtered through a silica plug, and the solvent was evaporated. Reversed phase preparative-HPLC gave 103 mg of the intermediate S-methylated imidazolthiol. To a solution of zinc iodide (522 mg, 1.63 mmol) in THF (2 mL) was added methylmagnesium bromide (0.545 mL, 1.63 mmol). To the formed slurry was then added the purified intermediate in THF (4 mL), followed by bis(triphenylphosphine)palladium(II) chloride (19 mg, 30 μ mol). The reaction mixture was stirred at 40 °C for 2 h. Reversed phase preparative-HPLC gave 29 mg of the intermediate aminoimidazole. The purified material, pyridin-3-ylboronic acid (21 mg, 0.17 mmol), and bis(triphenylphosphine)palladium(II) chloride (12 mg, 20 μ mol) were taken up in DME (1 mL) and water (0.5 mL). Sodium carbonate (1 M in water) (0.21 mL, 0.21 mmol) was added, and the mixture was heated at 80 °C for 2 h. Reversed phase preparative-HPLC gave 16 mg (1%, over four steps) of the title compound. ¹H NMR (400 MHz, methanol- d_4) δ ppm 8.74 (s, 1 H), 8.51 (d, $J = 4.55$ Hz, 1 H), 8.04 (d, $J = 8.08$ Hz, 1 H), 7.67 (s, 1 H), 7.57 (d, $J = 7.07$ Hz, 1 H), 7.38–7.53 (m, 5 H), 7.02 (t, $J = 8.72$ Hz, 2 H), 2.38 (s, 3 H); MS (ES+) m/z 345 [M + H]⁺.

2-(4-Methoxyphenyl)-5-methyl-2-(3-(pyrimidin-5-yl)phenyl)-2H-imidazol-4-amine (1j). To a solution of zinc iodide (13 g, 41 mmol) in THF (20 mL) at 0 °C was added methylmagnesium bromide (3 M in diethyl ether) (14 mL, 42 mmol). To the formed slurry was then added 2-(3-bromophenyl)-2-(4-methoxyphenyl)-5-(methylthio)-2H-imidazol-4-amine (10j) (1.6 g, 4.1 mmol) in THF (20 mL), followed by bis(triphenylphosphine)palladium(II) chloride (0.29 g, 0.41 mmol). The reaction mixture was stirred at 50 °C for 3 h. Methanol was added to quench the reaction, and the solvent was then evaporated. Water was added resulting in a thick slurry which was extracted with dichloromethane. The combined organic phases were dried (MgSO₄), filtered, and the solvent was evaporated. Silica column chromatography (0:1 → 1:0, EtOAc/dichloromethane) gave 0.88 g. A portion of the purified material (0.22 g), pyrimidin-5-ylboronic acid (95 mg, 0.76 mmol), and bis(triphenylphosphine)palladium(II) chloride (54 mg, 80 μ mol) were taken up in DME (3 mL) and water (1.5 mL). Sodium carbonate (1 M in water) (0.95 mL, 0.95 mmol) was added, and the mixture was heated at 80 °C for 2 h. Reversed phase preparative-HPLC gave 36 mg (1%, over two steps) of the title compound. ¹H NMR (400 MHz, chloroform- d_3) δ ppm 9.19 (s, 1 H), 8.93 (s, 2 H), 7.77 (s, 1 H), 7.61–7.70 (m, 1 H), 7.50 (d, $J = 8.84$ Hz, 2 H), 7.44 (d, $J = 5.05$ Hz, 2 H), 6.84 (d, $J = 8.84$ Hz, 2 H), 3.78 (s, 3 H), 2.36 (s, 3 H); MS (ES+) m/z 358 [M + H]⁺.

2-(4-Methoxyphenyl)-5-methyl-2-(3-(pyridin-3-yl)phenyl)-2H-imidazol-4-amine (1k). To a solution of zinc iodide (13 g, 41 mmol) in THF (20 mL) at 0 °C was added methylmagnesium bromide (3 M in diethyl ether) (14 mL, 42 mmol). To the formed slurry was then added 2-(3-bromophenyl)-2-(4-methoxyphenyl)-5-(methylthio)-2H-imidazol-4-amine (10j) (1.6 g, 4.1 mmol) in THF (20 mL), followed by bis(triphenylphosphine)palladium(II) chloride (0.29 g, 0.41 mmol). The reaction mixture was stirred at 50 °C for 3 h. Methanol was added to quench the reaction, and the solvent was then evaporated. Water was added resulting in a thick slurry which was extracted with dichloromethane. The combined organic phases were

dried (MgSO_4), filtered, and the solvent was evaporated. Silica column chromatography (0:1 \rightarrow 1:0, EtOAc/dichloromethane) gave 0.88 g. A portion the purified material (200 mg), pyridin-3-ylboronic acid (86 mg, 0.70 mmol), and bis(triphenylphosphine)palladium(II) chloride (49 mg, 70 μmol) were taken up in DME (2 mL) and water (1 mL). Sodium carbonate (1 M in water) (0.9 mL, 0.9 mmol) was added, and the mixture was heated at 80 °C for 2 h. Reversed phase preparative-HPLC gave 39 mg (1%, over two steps) of the title compound. ^1H NMR (400 MHz, chloroform- d_3) δ ppm 8.82 (d, $J = 1.77$ Hz, 1 H), 8.57 (dd, $J = 4.55, 1.26$ Hz, 1 H), 7.86 (ddd, $J = 7.96, 1.89, 1.77$ Hz, 1 H), 7.77 (s, 1 H), 7.60 (d, $J = 7.58$ Hz, 1 H), 7.50 (d, $J = 8.84$ Hz, 2 H), 7.37–7.47 (m, 2 H), 7.34 (dd, $J = 7.83, 4.80$ Hz, 1 H), 6.83 (d, $J = 8.84$ Hz, 2 H), 5.18 (br s, 2 H), 3.77 (s, 3 H), 2.35 (s, 3 H); MS (ES+) m/z 357 $[\text{M} + \text{H}]^+$.

2-(4-Methoxy-3-methylphenyl)-5-methyl-2-(3-(pyrimidin-5-yl)phenyl)-2H-imidazol-4-amine (11). 2-(3-Bromophenyl)-2-(4-methoxy-3-methylphenyl)-5-methyl-2H-imidazol-4-amine (71) (0.3 g, 0.8 mmol), pyrimidin-5-ylboronic acid (0.12 g, 0.97 mmol), [1,1'-bis(diphenylphosphino)ferrocene]palladium(II) chloride (33 mg, 40 μmol), potassium carbonate (2 M in water) (1.2 mL, 2.4 mmol), and dioxane (4 mL) were mixed in a vial and heated in a microwave reactor at 130 °C for 15 min. The mixture was diluted with methanol (5 mL), filtered, and purified by reversed phase preparative-HPLC to give 0.14 g (46%) the title compound. ^1H NMR (500 MHz, DMSO- d_6) δ ppm 2.08 (s, 3H), 2.24 (s, 3), 3.71 (s, 3H), 6.61 (br s, 2H), 6.79 (d, $J = 8.51$ Hz, 1H), 7.29–7.50 (m, 3H), 7.50–7.70 (m, 2H), 7.82 (t, $J = 1.73$ Hz, 1H), 9.01 (s, 2H), 9.19 (s, 1H); MS (ES+) m/z 372 $[\text{M} + \text{H}]^+$.

2-(4-Methoxy-3,5-dimethylphenyl)-5-methyl-2-(3-(pyrimidin-5-yl)phenyl)-2H-imidazol-4-amine (1m). 1,3-Dibromobenzene (3.0 mL, 25 mmol) was dissolved in diethyl ether (60 mL) and cooled to -78 °C. *n*-Butyllithium (2.5 M in hexane) (10 mL, 25 mmol) was added and the solution stirred for 30 min. 4-Methoxy-3,5-dimethylbenzonitrile (4.06 g, 25.20 mmol) was added in diethyl ether (40 mL) at -78 °C, and the mixture was allowed to warm to room temperature over 30 min. Methanol (20 mL) containing ammonium acetate (2 g, 26 mmol) was added. The solvents were evaporated, and the residue was taken up in dichloromethane and water. The organic layer was separated and the water phase extracted with dichloromethane. The combined organic phases were shaken with brine and dried (MgSO_4), filtered, and the solvent was evaporated. The intermediate imine and ethanebis(thioamide) (2.91 g, 24.20 mmol) were taken up in ethanol (10 mL). The mixture was heated at 165 °C for 2 h by microwave irradiation. The solvent was evaporated and the residue subjected to silica column chromatography (0:1 \rightarrow 1:0, EtOAc/heptane) to give the intermediate imidazothiol. The purified intermediate was taken up in THF (20 mL). Iodomethane (1.0 mL, 16 mmol) was added, and the mixture was heated at 60 °C for 24 h. The cooled solution was then subjected to silica column chromatography (0:1 \rightarrow 1:0, EtOAc/heptane) to give the intermediate S-methylated imidazothiol. To a solution of zinc iodide (11 g, 35 mmol) in THF (40 mL) at 0 °C was added methylmagnesium bromide (3 M in diethyl ether) (11.6 mL, 34.8 mmol). To the formed slurry was then added the purified intermediate in THF (20 mL), followed by bis(triphenylphosphine)palladium(II) chloride (0.31 g, 0.44 mmol). The reaction mixture was stirred at 50 °C for 3 h. The reaction mixture was filtered, and the solids were rinsed with dichloromethane. The organic phase was dried (MgSO_4), filtered, and the solvent was evaporated. Silica column chromatography (0:1 \rightarrow 1:0, 10% acetic acid in EtOAc/dichloromethane) gave 0.4 g of the intermediate aminoimidazole. A portion of the purified material (270 mg), pyrimidin-5-ylboronic acid (0.17 g, 1.4 mmol), and bis(triphenylphosphine)palladium(II) chloride (98 mg, 0.14 mmol) were taken up in DME (8 mL) and water (4 mL). Sodium carbonate (1 M in water) (1.7 mL, 1.7 mmol) was added, and the mixture was heated at 80 °C for 2 h. The reaction mixture was extracted with dichloromethane. The combined organic phases were dried (MgSO_4), filtered, and the solvent was evaporated. Reversed phase preparative-HPLC gave 88 mg (1%, over five steps) of the title compound. ^1H NMR (400 MHz, methanol- d_4) δ ppm 9.12 (s, 1 H), 9.02 (s, 2 H), 7.70 (s, 1 H), 7.62 (d, $J = 7.58$ Hz, 1

H), 7.51–7.56 (m, 1 H), 7.43–7.51 (m, 1 H), 7.04 (s, 2 H), 3.66 (s, 3 H), 2.37 (s, 3 H), 2.21 (s, 6 H); MS (ES+) m/z 386 $[\text{M} + \text{H}]^+$.

(S)-2-(4-Methoxy-3,5-dimethylphenyl)-5-methyl-2-(3-(pyrimidin-5-yl)phenyl)-2H-imidazol-4-amine and (R)-2-(4-Methoxy-3,5-dimethylphenyl)-5-methyl-2-(3-(pyrimidin-5-yl)phenyl)-2H-imidazol-4-amine ((S)-1m and (R)-1m). 2-(3-Bromophenyl)-2-(4-methoxy-3,5-dimethylphenyl)-5-methyl-2H-imidazol-4-amine (0.27 g, 0.70 mmol), pyrimidin-5-ylboronic acid (0.17 g, 1.4 mmol), and bis(triphenylphosphine)palladium(II) chloride (98 mg, 0.14 mmol) were taken up in DME (8 mL) and water (4 mL). Sodium carbonate (1 M in water) (1.7 mL, 1.7 mmol) was added, and the mixture was heated at 80 °C for 2 h. The solvent was evaporated, and the residue was dissolved in methanol (7.5 mL). The resulting solution was injected (15 stacked injections) on a Chiralpak AD-H column (21.2 mm \times 250 mm), using methanol/ CO_2 (10:90) + 0.1% DEA as eluent at a flow rate of 50 mL/min. The (S)-enantiomer was the first to elute and was concentrated in vacuo to give 30 mg (11%). ^1H NMR (400 MHz, methanol- d_4) δ ppm 9.12 (s, 1 H), 9.02 (s, 2 H), 7.70 (s, 1 H), 7.62 (d, $J = 7.58$ Hz, 1 H), 7.51–7.56 (m, 1 H), 7.43–7.51 (m, 1 H), 7.04 (s, 2 H), 3.66 (s, 3 H), 2.37 (s, 3 H), 2.21 (s, 6 H); MS (ES+) m/z 386 $[\text{M} + \text{H}]^+$. The (R)-enantiomer was the second to elute and was concentrated in vacuo to give 29 mg (11%). ^1H NMR (400 MHz, methanol- d_4) δ ppm 9.12 (s, 1 H), 9.02 (s, 2 H), 7.70 (s, 1 H), 7.62 (d, $J = 7.58$ Hz, 1 H), 7.51–7.56 (m, 1 H), 7.43–7.51 (m, 1 H), 7.04 (s, 2 H), 3.66 (s, 3 H), 2.37 (s, 3 H), 2.21 (s, 6 H); MS (ES+) m/z 386 $[\text{M} + \text{H}]^+$.

2-(4-Methoxy-3,5-dimethylphenyl)-5-methyl-2-{3-[5-(prop-1-yn-1-yl)pyridin-3-yl]phenyl}-2H-imidazol-4-amine (1n). To a solution of 2-(3-bromophenyl)-2-(4-methoxy-3,5-dimethylphenyl)-5-methyl-2H-imidazol-4-amine (0.12 g, 0.31 mmol) in dioxane/ethanol/ H_2O (2 mL/0.5 mL/0.5 mL) were added [5-(prop-1-yn-1-yl)pyridin-3-yl]boronic acid (75 mg, 0.47 mmol), sodium carbonate (66 mg, 0.62 mmol), tris(dibenzylideneacetone)dipalladium(0) (12 mg), and 4,5-bis(diphenylphosphino)-9,9-dimethylxanthene (12 mg) under nitrogen atmosphere. The mixture was stirred at 100 °C overnight. Water (5 mL) was added, and the mixture was extracted with EtOAc. The combined organic layers were dried (MgSO_4) and concentrated to give the product, which was purified by reversed phase preparative-HPLC to give 26 mg (20%) of the title compound. ^1H NMR (400 MHz, chloroform- d_3) δ ppm 8.69 (d, $J = 2.0$ Hz, 1 H), 8.57 (d, $J = 1.6$ Hz, 1 H), 7.87 (s, 1 H), 7.76 (s, 1 H), 7.62 (d, $J = 7.2$ Hz, 1 H), 7.39–7.46 (m, 2 H), 7.19 (s, 2 H), 3.67 (s, 3 H), 2.37 (s, 3 H), 2.24 (s, 6 H), 2.06 (s, 3 H); MS (ES+) 423.2 $[\text{M} + \text{H}]^+$.

2-Benzyl-5-methyl-2-(3-(pyrimidin-5-yl)phenyl)-2H-imidazol-4-amine ((S)-1o and (R)-1o). 1-(3-Bromophenyl)-2-phenylethanone (1.0 g, 3.6 mmol) and ethanebis(thioamide) (1.3 g, 11 mmol) were taken up in ammonia (7 M in methanol) (15 mL, 0.11 mmol). The mixture was heated at 150 °C for 1 h by microwave irradiation. The reaction mixture was diluted with dichloromethane and filtered. Silica column chromatography (0:1 \rightarrow 1:0, EtOAc/heptane) gave 1.23 g of the intermediate imidazothiol. The purified material was taken up in THF (30 mL). Iodomethane (0.64 mL, 10.3 mmol) was added, and the mixture was heated at 60 °C for 4 h. Silica column chromatography using (0:1 \rightarrow 1:0, EtOAc/heptane) gave 200 mg of the intermediate S-methylated intermediate imidazothiol. The purified intermediate and 1,3-bis(diphenylphosphino)propanenickel(II) chloride (0.12 mg, 0.21 mmol) were dissolved in toluene (3 mL). Methylmagnesium bromide (3 M in diethyl ether) (1.4 mL, 4.2 mmol) was added and the resulting suspension stirred at room temperature. After 1 h water was added and the phases were separated. The water phase was extracted with dichloromethane. The combined organic phases were dried (MgSO_4), filtered and the solvents evaporated. Reversed phase preparative-HPLC gave 67 mg of the intermediate aminoimidazole. The purified material, pyrimidin-5-ylboronic acid (48 mg, 0.39 mmol), and bis(triphenylphosphine)palladium(II) chloride (27 mg, 40 μmol) were taken up in DME (1 mL) and water (0.5 mL). Sodium carbonate (1 M in water) (0.5 mL, 0.5 mmol) was added, and the mixture was heated at 80 °C for 2 h. The reaction mixture was extracted with dichloromethane. The combined organic phases were dried (MgSO_4), filtered, and the solvent was evaporated. Reversed

phase preparative-HPLC gave 30 mg of the title compound. The purified material was dissolved in methanol (2.7 mL), and the resulting solution was injected (three stacked injections) on a LuxC2 column (21.2 mm × 250 mm), using methanol/CO₂ (18:82) + 0.1% DEA as eluent at a flow rate of 50 mL/min. The (*S*)-enantiomer was the first to elute and was concentrated in vacuo to give 8 mg (0.6%, over four steps). ¹H NMR (400 MHz, methanol-*d*₄) δ ppm 2.07 (s, 3 H), 3.33–3.50 (m, 2 H), 7.00–7.09 (m, 2 H), 7.11–7.21 (m, 3 H), 7.49–7.56 (m, 1 H), 7.62–7.68 (m, 1 H), 7.76 (dt, *J* = 7.83, 1.26 Hz, 1 H), 7.90 (t, *J* = 1.77 Hz, 1 H), 9.05 (s, 2 H), 9.14 (s, 1 H); MS (ES+) *m/z* 342 [M + H]⁺. The (*R*)-enantiomer was the second to elute and was concentrated in vacuo to give 8 mg (0.6%, over four steps). ¹H NMR (400 MHz, methanol-*d*₄) δ ppm 2.07 (s, 3 H), 3.33–3.50 (m, 2 H), 7.00–7.09 (m, 2 H), 7.11–7.21 (m, 3 H), 7.49–7.56 (m, 1 H), 7.62–7.68 (m, 1 H), 7.76 (dt, *J* = 7.83, 1.26 Hz, 1 H), 7.90 (t, *J* = 1.77 Hz, 1 H), 9.05 (s, 2 H), 9.14 (s, 1 H); MS (ES+) *m/z* 342 [M + H]⁺.

2-(3-(5-Chloropyridin-3-yl)phenyl)-2-cyclopropyl-5-methyl-2H-imidazol-4-amine (1p). The title compound was prepared as described for compound **1l** in 52% yield starting with 5-chloropyridin-3-ylboronic acid (68 mg, 0.43 mmol) and 2-(3-bromophenyl)-2-cyclopropyl-5-methyl-2H-imidazol-4-amine (**7p**) (90 mg, 0.31 mmol). ¹H NMR (500 MHz, DMSO-*d*₆) δ ppm -0.01 to 0.07 (m, 1H), 0.17–0.26 (m, 1H), 0.27–0.39 (m, 2H), 1.56–1.64 (m, 1H), 2.16 (s, 3H), 6.50 (br s, 2H), 7.40–7.46 (m, 1H), 7.65 (d, *J* = 7.65 Hz, 1H), 7.62 (d, *J* = 7.72 Hz, 1H), 7.88 (br s, 1H), 8.15 (br s, 1H), 8.63 (d, *J* = 1.89 Hz, 1H), 8.78 (br. s, 1H); MS (ES+) *m/z* 325 [M + H]⁺.

2-Cyclohexyl-5-methyl-2-(3-(pyridin-3-yl)phenyl)-2H-imidazol-4-amine (1q). 1,3-Dibromobenzene (3.0 mL, 25 mmol) was dissolved in diethyl ether (60 mL) and cooled to -78 °C. *n*-Butyllithium (2.5 M in hexane) (10 mL, 25 mmol) was added and the solution stirred for 30 min. Cyclohexanecarbonitrile (3.0 mL, 25 mmol) was added in diethyl ether (40 mL) at -78 °C, and the mixture was allowed to warm to room temperature over 30 min. Methanol (20 mL) containing ammonium acetate (2 g, 26 mmol) was added. The solvents were evaporated, and the residue was taken up in dichloromethane and water. The organic layer was separated and the water phase extracted with dichloromethane. The combined organic phases were shaken with brine, dried (MgSO₄), and filtered and the solvent was evaporated to give the intermediate imine. The product and ethanebis(thioamide) (1.5 g, 12 mmol) were taken up in ethanol (10 mL). The mixture was heated at 165 °C for 2 h by microwave irradiation. The solvent was evaporated. Silica column chromatography (0:1 → 1:0 EtOAc/heptane) gave the intermediate imidazothiol. The purified material was taken up in THF (20 mL). Iodomethane (0.7 mL, 11 mmol) was added, and the mixture was heated at 60 °C for 24 h. Silica column chromatography (0:1 → 1:0 EtOAc/heptane) gave the intermediate *S*-methylated imidazothiol. To a solution of zinc iodide (5 g, 16 mmol) in THF (40 mL) at 0 °C was added methylmagnesium bromide (3 M in diethyl ether) (5.3 mL, 16 mmol). To the formed slurry was then added the purified intermediate (0.93 g, 2.5 mmol) in THF (20 mL), followed by bis(triphenylphosphine)-palladium(II) chloride (0.18 g, 0.25 mmol). The reaction mixture was stirred at 50 °C for 3 h. Methanol was added to quench the reaction. The solvent was evaporated. Water was added resulting in a thick slurry which was washed with dichloromethane. The combined organic phases were dried (MgSO₄), filtered, and the solvent was evaporated. Reversed phase preparative-HPLC gave 0.12 g of the intermediate aminoimidazole. A portion of the purified intermediate (60 mg), pyridin-3-ylboronic acid (44 mg, 0.36 mmol), and bis(triphenylphosphine)palladium(II) chloride (25 mg, 40 μmol) were taken up in DME (2 mL) and water (1 mL). Sodium carbonate (1 M in water) (0.45 mL, 0.45 mmol) was added and the mixture was heated at 80 °C for 2 h. Reversed phase preparative-HPLC gave 28 mg (0.7%, over five steps) of the title compound. ¹H NMR (400 MHz, chloroform-*d*₃) δ ppm 8.87 (d, *J* = 2.02 Hz, 1 H), 8.58 (dd, *J* = 4.80, 1.52 Hz, 1 H), 7.92 (ddd, *J* = 7.96, 1.89, 1.77 Hz, 1 H), 7.84 (s, 1 H), 7.66 (d, *J* = 7.33 Hz, 1 H), 7.46–7.52 (m, 1 H), 7.40–7.46 (m, 1 H), 7.35 (dd, *J* = 7.71, 4.93 Hz, 1 H), 5.50 (br s, 2 H), 2.30 (s, 3 H), 2.06–2.17 (m, 1 H), 1.42–1.77 (m, 5 H), 0.86–1.25 (m, 5 H); MS (ES+) *m/z* 333 [M + H]⁺.

2-(3'-Methoxybiphenyl-3-yl)-5-methyl-2-(tetrahydro-2H-pyran-4-yl)-2H-imidazol-4-amine (1r). 1,3-Dibromobenzene (3.0 mL, 25 mmol) was dissolved in diethyl ether (60 mL) and cooled to -78 °C. *n*-Butyllithium (2.5 M in hexane) (10 mL, 25 mmol) was added and the solution stirred for 30 min. Tetrahydro-2H-pyran-4-carbonitrile (2.8 g, 25 mmol) was added in diethyl ether (20 mL) at -78 °C, and the mixture was stirred for 30 min. The mixture was then allowed to reach room temperature over 30 min. Methanol (20 mL) containing ammonium acetate (2.0 g, 26 mmol) was added. The solvents were evaporated, and the residue was taken up in dichloromethane and water. The organic layer was separated and the water phase extracted with dichloromethane. The combined organic phases were shaken with brine and dried (MgSO₄). The mixture was filtered and the solvent evaporated to give 4.6 g of the intermediate imine. The material and ethanebis(thioamide) (2.5 g, 21 mmol) were taken up in ethanol (10 mL). The mixture was heated at 165 °C for 2 h by microwave irradiation. The reaction mixture was diluted with dichloromethane and filtered. Silica column chromatography (0:1 → 1:0 EtOAc/heptane) gave 3.7 g of the intermediate imidazothiol. The purified material was taken up in THF (20 mL). Iodomethane (2.0 mL, 31 mmol) was added, and the mixture was heated at 60 °C for 24 h. Silica column chromatography (0:1 → 1:0 EtOAc/heptane) gave 2.2 g of the intermediate *S*-methylated imidazothiol. A portion of the purified material (0.63 g), 3-methoxyphenylboronic acid (0.26 g, 1.7 mmol), and bis(triphenylphosphine)palladium(II) chloride (0.12 g, 0.17 mmol) were taken up in DME (20 mL) and water (10 mL). Sodium carbonate (1 M in water) (4.2 mL, 4.2 mmol) was added, and the mixture was heated at 80 °C for 2 h. The reaction mixture was extracted with dichloromethane. The combined organic phases were dried (MgSO₄), filtered and the solvents evaporated. Reversed phase preparative-HPLC gave 80 mg of intermediate arylated *S*-methylated imidazothiol. To a solution of zinc iodide (0.65 g, 2.0 mmol) in THF (10 mL) at 0 °C was added methylmagnesium bromide (3 M in diethyl ether) (0.7 mL, 2.1 mmol). To the formed slurry was then added bis(triphenylphosphine)palladium(II) chloride (28 mg, 40 μmol) followed by the purified intermediate in THF (5 mL). The reaction mixture was stirred at 80 °C for 3 h. Methanol was added to quench the reaction. Saturated NH₄Cl solution was added, and the mixture was extracted with dichloromethane. The combined organic phases were dried (MgSO₄), filtered, and the solvent was evaporated. Reversed phase preparative-HPLC gave 18 mg (0.2%, over five steps) of the title compound. ¹H NMR (400 MHz, methanol-*d*₄) δ ppm 7.79 (s, 1 H), 7.59–7.68 (m, 1 H), 7.47–7.58 (m, 3 H), 7.38 (t, *J* = 7.83 Hz, 1 H), 7.33 (t, *J* = 7.83 Hz, 1 H), 7.18 (d, *J* = 7.83 Hz, 1 H), 7.15 (d, *J* = 2.02 Hz, 1 H), 6.90 (dd, *J* = 8.08, 2.02 Hz, 1 H), 3.87 (d, *J* = 11.37 Hz, 2 H), 3.84 (s, 3 H), 3.24–3.37 (m, 2 H), 2.35–2.47 (m, 1 H), 2.32 (s, 3 H), 1.22–1.43 (m, 4 H); MS (ES+) *m/z* 364 [M + H]⁺.

1-(4-(4-Amino-2-(3'-methoxybiphenyl-3-yl)-5-methyl-2H-imidazol-2-yl)piperidin-1-yl)ethanone (1s). 1,3-Dibromobenzene (1.4 mL, 12 mmol) was dissolved in diethyl ether (90 mL) and cooled to -78 °C. *n*-Butyllithium (2.5 M in hexane) (5 mL, 12.5 mmol) was added and the solution stirred for 30 min. *tert*-Butyl 4-cyanopiperidine-1-carboxylate (2.5 g, 12 mmol) was added in diethyl ether (40 mL) at -78 °C. The mixture was stirred for 30 min and was then allowed to warm to room temperature over 30 min. Methanol (20 mL) containing ammonium acetate (1 g, 13 mmol) was added. The solvents were evaporated, and the residue was taken up in dichloromethane and water. The organic layer was separated and the water phase extracted with dichloromethane. The combined organic phases were shaken with brine, dried (MgSO₄), and filtered and the solvent was evaporated to give 2.9 g of the intermediate imine. A portion of the material (2.65 g) and ethanebis(thioamide) (1.0 g, 8.3 mmol) were taken up in ethanol (10 mL). The mixture was heated at 180 °C for 30 min by microwave irradiation. The reaction mixture was diluted with dichloromethane and filtered. Silica column chromatography (0:1 → 1:0 EtOAc/heptane) gave 0.94 g of the intermediate imidazothiol. The purified material was taken up in THF (20 mL). Iodomethane (0.39 mL, 6.2 mmol) was added, and the mixture was heated at 60 °C for 24 h. Silica column chromatography (0:1 → 1:9 0.1% ammonia in methanol/dichloromethane) gave 0.57 g of the

intermediate S-methylated imidazothiol. To a solution of zinc iodide (3.4 g, 10.7 mmol) in THF (20 mL) at 0 °C was added methylmagnesium bromide (3 M in diethyl ether) (3.6 mL, 10.7 mmol). To the formed slurry was then added bis-(triphenylphosphine)palladium(II) chloride (0.15 g, 0.21 mmol) followed by the purified intermediate in THF (10 mL). The mixture was stirred at 50 °C for 3 h. Methanol was added to quench the reaction. Saturated NH₄Cl solution was added, and the mixture was extracted with diethyl ether. The combined organic phases were dried (MgSO₄), filtered, and the solvent was evaporated. Reversed phase preparative-HPLC gave 45 mg of the intermediate aminoimidazole. The purified material, 3-methoxyphenylboronic acid (18 mg, 0.12 mmol), and bis(triphenylphosphine)palladium(II) chloride (7 mg, 10 μmol) were taken up in DME (1 mL) and water (0.5 mL). Sodium carbonate (1 M in water) (0.26 mL, 0.26 mmol) was added, and the mixture was heated at 80 °C for 2 h. The reaction mixture was filtered, and reversed phase preparative-HPLC gave 16 mg of the intermediate arylated aminoimidazole. The purified material was dissolved in dichloromethane (2 mL). Trifluoroacetic acid (1.0 mL, 13 mmol) was added, and the mixture was stirred at room temperature for 1 h. The solvent and excess reagent were evaporated. The residue was dissolved in dichloromethane (2 mL) and triethylamine (11 μL, 80 μmol). Acetic anhydride (4 μL, 40 μmol) was added, and the mixture was stirred for 16 h. The solvent was evaporated and reversed phase preparative-HPLC gave 12 mg (0.3%, over seven steps) of the title compound. ¹H NMR (400 MHz, methanol-*d*₄) δ ppm 7.80 (br s, 1 H), 7.53 (d, *J* = 7.58 Hz, 2 H), 7.39 (t, *J* = 7.45 Hz, 1 H), 7.34 (t, *J* = 7.96 Hz, 1 H), 7.18 (d, *J* = 7.83 Hz, 1 H), 7.16 (s, 1 H), 6.91 (dd, *J* = 8.21, 1.89 Hz, 1 H), 4.49 (d, *J* = 12.88 Hz, 1 H), 3.79–3.92 (m, 4 H), 2.90–3.06 (m, 1 H), 2.39–2.54 (m, 2 H), 2.33 (br s, 3 H), 2.03 (s, 3 H), 1.36–1.62 (m, 2 H), 1.25 (d, *J* = 11.87 Hz, 1 H), 0.99–1.17 (m, 1 H); MS (ES+) *m/z* 405 [M + H]⁺.

2-Cyclopropyl-5-methyl-2-(3-(5-(prop-1-ynyl)pyridin-3-yl)phenyl)-2H-imidazol-4-amine (1t). The title compound was prepared as described for compound 11 in 40% yield starting with 5-(prop-1-ynyl)pyridin-3-ylboronic acid (917471–30–8) (86 mg, 0.53 mmol) and 2-(3-bromophenyl)-2-cyclopropyl-5-methyl-2H-imidazol-4-amine (7p) (78 mg, 0.27 mmol). ¹H NMR (500 MHz, DMSO-*d*₆) δ ppm –0.02–0.07 (m, 1H), 0.16–0.26 (m, 1H), 0.27–0.39 (m, 2H), 1.55–1.62 (m, 1H), 2.12 (s, 3H), 2.16 (s, 3H), 6.50 (br s, 2H), 7.41 (t, *J* = 7.72 Hz, 1H), 7.59 (d, *J* = 7.65 Hz, 1H), 7.64 (d, *J* = 7.72 Hz, 1H), 7.85 (br s, 1H), 7.98 (br s, 1H), 8.58 (br s, 1H), 8.73–8.77 (m, 1H); MS (ES+) *m/z* 329 [M + H]⁺.

4-(4-Amino-2-cyclopropyl-5-methyl-2H-imidazol-2-yl)-2-(5-(prop-1-ynyl)pyridin-3-yl)phenol (1u). The title compound was prepared as described for compound 11 in 28% yield starting with 4-(4-amino-2-cyclopropyl-5-methyl-2H-imidazol-2-yl)-2-bromophenol (14) (60 mg, 0.19 mmol) and 5-(prop-1-ynyl)pyridin-3-ylboronic acid (47 mg, 0.29 mmol). ¹H NMR (500 MHz, DMSO-*d*₆) δ ppm –0.07 to 0.03 (m, 1H), 0.14–0.23 (m, 1H), 0.24–0.33 (m, 2H), 1.44–1.52 (m, 1H), 2.10 (s, 3H), 2.13 (s, 3H), 6.41 (br s, 2H), 6.88 (d, *J* = 8.51 Hz, 1H), 7.42 (dd, *J* = 8.35, 2.21 Hz, 1H), 7.45 (d, *J* = 2.21 Hz, 1H), 7.85 (t, *J* = 2.05 Hz, 1H), 8.50 (d, *J* = 1.89 Hz, 1H), 8.61 (d, *J* = 2.05 Hz, 1H), 9.72 (br s, 1H); MS (ES+) *m/z* 345 [M + H]⁺.

4-(4-Amino-2-cyclopropyl-5-methyl-2H-imidazol-2-yl)-2-(4-(prop-1-ynyl)pyridin-2-yl)phenol (1v). 2-Cyclopropyl-2-(4-methoxy-3-(4-(prop-1-ynyl)pyridin-2-yl)phenyl)-5-methyl-2H-imidazol-4-amine (15) (16 mg, 40 μmol) was dissolved in dichloromethane (1.0 mL) and cooled to –78 °C. Boron tribromide (15 μL, 0.16 mmol) was added dropwise, and the reaction mixture was slowly warmed to room temperature overnight. The reaction was quenched by dropwise addition of methanol (0.5 mL). Then ammonia (35% in water) (0.5 mL) was added. HCl (2 M) was added dropwise until pH 7 was obtained. The organics were evaporated, and the resulting residue was taken up in dichloromethane. The organic layer was collected and the water phase was extracted with dichloromethane. The combined organic layers were dried (Na₂SO₄), filtered, and concentrated. Purification by reversed phase preparative HPLC gave 2 mg (14%) of the title compound. ¹H NMR (500 MHz, DMSO-*d*₆) δ ppm 13.21 (s, 1H), 8.58 (d, *J* = 5.04 Hz, 1H), 8.07 (d, *J* = 2.21 Hz, 1H), 7.94 (s,

1H), 7.50 (dd, *J* = 8.51, 2.21 Hz, 1H), 7.37 (dd, *J* = 5.20, 1.10 Hz, 1H), 6.85 (d, *J* = 8.51 Hz, 1H), 6.45 (br s, 2H), 2.16 (s, 3H), 2.15 (s, 3H), 1.53 (tt, *J* = 8.04, 5.20 Hz, 1H), 0.25–0.36 (m, 2H), 0.13–0.24 (m, 1H), –0.05 to 0.05 (m, 1H); MS (ES+) *m/z* 345 [M + H]⁺.

■ ASSOCIATED CONTENT

Supporting Information

Synthetic procedures and analytical data for intermediates 2, 3l,p, 4h,i,l, 6c,b, 7b,l,p, 9j, 10j, 6a, 11–15 (intermediates named after the corresponding compounds 1); Table 1 listing crystallographic data; Figures 1 and 2 showing compounds bound to BACE-1 active site. This material is available free of charge via the Internet at <http://pubs.acs.org>.

Accession Codes

New protein/ligand coordinates for (S)-1m and (R)-1t have been deposited in the PDB with codes 4b1d and 4b1c, respectively.

■ AUTHOR INFORMATION

Corresponding Author

*Phone: +46 (0) 70 672 48 97. E-mail: ylva.gravenfors@hotmail.com.

Present Address

¹Sprint Bioscience Teknikringen 38A, SE-114 28 Stockholm, Sweden. Phone: +46 (0)70 497 41 18. E-mail: fredrik.rahm@sprintbioscience.com.

Notes

The authors declare no competing financial interest.

■ ACKNOWLEDGMENTS

We thank the Physicochemical Characterization Team and the Analytical and Purification Sciences Team at the Department of Medicinal Chemistry at AstraZeneca Södertälje, Sweden, for physicochemical characterization, enantiomer separations, and purity determinations. We thank Martin Levin for FRET and sAPPβ measurements. We thank Carolina Sandman and Carrie Tsoi for Caco-2 measurements, Eva Spennare and Jenny Johansson for determination of the fraction unbound in brain and plasma protein binding, Sveinn Briem and the team for bioanalysis, and the following people involved in performing the in vivo experiments: Daniel Bergström, Ann Staflund, Anette Stålebring Löwstedt, Susanne Gustavsson, and Carina Stephan. In addition, we thank Anna Aagaard for crystallization, and we thank Safety Assessment Screening Centre at AstraZeneca Alderly Park for hERG assessments.

■ ABBREVIATIONS USED

Aβ, amyloid-β; AD, Alzheimer's disease; APP, amyloid-β precursor protein; BACE, β-site amyloid-β precursor protein cleaving enzyme; cPr, cyclopropyl; DEA, diethylamine; ER, efflux ratio; IPA, isopropanol; iv, intravenous; PD, pharmacodynamic; P-gp, permeability glycoprotein; po, per oral; PSA, polar surface area; sAPPβ, soluble amyloid-β precursor protein; SAR, structure–activity relationship; TEA, triethylamine

■ REFERENCES

- (1) Querfurth, H. W.; LaFerla, F. M. Alzheimer's disease. *N. Engl. J. Med.* **2010**, *362*, 329–344.
- (2) 2012 Alzheimer's disease facts and figures. *Alzheimer's Dementia* **2012**, *8*, 131–168.
- (3) Hardy, J.; Allsop, D. Amyloid deposition as the central event in the etiology of Alzheimer's disease. *Trends Pharmacol. Sci.* **1991**, *12*, 383–388.

- (4) Lee, V. M.; Goedert, M.; Trojanowski, J. Q. Neurodegenerative tauopathies. *Annu. Rev. Neurosci.* **2001**, *24*, 1121–1159.
- (5) Hardy, J.; Selkoe, D. J. The amyloid hypothesis of Alzheimer's disease: progress and problems on the road to therapeutics. *Science (Washington, DC, U. S.)* **2002**, *297*, 353–356.
- (6) Hussain, I.; Powell, D.; Howlett, D. R.; Tew, D. G.; Meek, T. D.; Chapman, C.; Gloger, I. S.; Murphy, K. E.; Southan, C. D.; Ryan, D. M.; Smith, T. S.; Simmons, D. L.; Walsh, F. S.; Dingwall, C.; Christie, G. Identification of a novel aspartic protease (Asp 2) as β -secretase. *Mol. Cell. Neurosci.* **1999**, *14*, 419–427.
- (7) Sinha, S.; Anderson, J. P.; Barbour, R.; Basi, G. S.; Caccavello, R.; Davis, D.; Doan, M.; Dovey, H. F.; Frigon, N.; Hong, J.; Jacobson-Croak, K.; Jewett, N.; Keim, P.; Knops, J.; Lieberburg, I.; Power, M.; Tan, H.; Tatsuno, G.; Tung, J.; Schenk, D.; Seubert, P.; Suomensaari, S. M.; Wang, S.; Walker, D.; Zhao, J.; McConlogue, L.; John, V. Purification and cloning of amyloid precursor protein β -secretase from human brain. *Nature (London)* **1999**, *402*, 537–540.
- (8) Vassar, R.; Bennett, B. D.; Babu-Khan, S.; Kahn, S.; Mendiaz, E. A.; Denis, P.; Teplow, D. B.; Ross, S.; Amarante, P.; Loeloff, R.; Luo, Y.; Fisher, S.; Fuller, J.; Edenson, S.; Lile, J.; Jarosinski, M. A.; Biere, A. L.; Curran, E.; Burgess, T.; Louis, J.; Collins, F.; Treanor, J.; Rogers, G.; Citron, M. β -Secretase cleavage of Alzheimer's amyloid precursor protein by the transmembrane aspartic protease BACE. *Science (Washington, DC, U. S.)* **1999**, *286*, 735–741.
- (9) Yan, R.; Bienkowski, M. J.; Shuck, M. E.; Miao, H.; Tory, M. C.; Pauley, A. M.; Brashler, J. R.; Stratman, N. C.; Mathews, W. R.; Buhl, A. E.; Carter, D. B.; Tomasselli, A. G.; Parodi, L. A.; Heinrichson, R. L.; Gurney, M. E. Membrane-anchored aspartyl protease with Alzheimer's disease β -secretase activity. *Nature (London)* **1999**, *402*, 533–537.
- (10) Lin, X.; Koelsch, G.; Wu, S.; Downs, D.; Dashti, A.; Tang, J. Human aspartic protease memapsin 2 cleaves the β -secretase site of β -amyloid precursor protein. *Proc. Natl. Acad. Sci. U.S.A.* **2000**, *97*, 1456–1460.
- (11) Price, D. L.; Sisodia, S. S. Mutant genes in familial Alzheimer's disease and transgenic models. *Annu. Rev. Neurosci.* **1998**, *21*, 479–505.
- (12) Hardy, J. A.; Higgins, G. A. Alzheimer's disease: the amyloid cascade hypothesis. *Science (Washington, DC, U. S.)* **1992**, *256*, 184–185.
- (13) Albert, J. S. Progress in the development of β -secretase inhibitors for Alzheimer's disease. *Prog. Med. Chem.* **2009**, *48*, 133–161.
- (14) Evin, G.; Lessene, G.; Wilkins, S. BACE inhibitors as potential drugs for the treatment of Alzheimer's disease: focus on bioactivity. *Recent Pat. CNS Drug Discovery* **2011**, *6*, 91–106.
- (15) Probst, G.; Xu, Y. Small-molecule BACE1 inhibitors: a patent literature review (2006–2011). *Expert Opin. Ther. Pat.* **2012**, *22*, 511–540.
- (16) Ghosh, A. K.; Shin, D.; Downs, D.; Koelsch, G.; Lin, X.; Ermolieff, J.; Tang, J. Design of potent inhibitors for human brain memapsin 2 (β -secretase). *J. Am. Chem. Soc.* **2000**, *122*, 3522–3523.
- (17) Cumming, J. N.; Iserloh, U.; Kennedy, M. E. Design and development of BACE-1 inhibitors. *Curr. Opin. Drug Discovery Dev.* **2004**, *7*, 536–556.
- (18) Malamas, M. S.; Erdei, J.; Gunawan, I.; Turner, J.; Hu, Y.; Wagner, E.; Fan, K.; Chopra, R.; Olland, A.; Bard, J.; Jacobsen, S.; Magolda, R. L.; Pangalos, M.; Robichaud, A. J. Design and synthesis of 5,5'-disubstituted aminohydantoin as potent and selective human β -secretase (BACE1) inhibitors. *J. Med. Chem.* **2010**, *53*, 1146–1158.
- (19) Swahn, B.; Holenz, J.; Kihlstrom, J.; Kolmodin, K.; Lindstrom, J.; Plobbeck, N.; Rotticci, D.; Sehgelmeble, F.; Sundstrom, M.; Berg, S. v.; Falting, J.; Georgievskaja, B.; Gustavsson, S.; Neelissen, J.; Ek, M.; Olsson, L.; Berg, S. Aminoimidazoles as BACE-1 inhibitors: the challenge to achieve in vivo brain efficacy. *Bioorg. Med. Chem. Lett.* **2012**, *22*, 1854–1859.
- (20) May, P. C.; Dean, R. A.; Lowe, S. L.; Martenyi, F.; Sheehan, S. M.; Boggs, L. N.; Monk, S. A.; Mathes, B. M.; Mergott, D. J.; Watson, B. M.; Stout, S. L.; Timm, D. E.; LaBell, E. S.; Gonzales, C. R.; Nakano, M.; Jhee, S. S.; Yen, M.; Ereshefsky, L.; Lindstrom, T. D.; Calligaro, D. O.; Cocke, P. J.; Hall, D. G.; Friedrich, S.; Citron, M.; Audia, J. E. Robust central reduction of amyloid- β in humans with an orally available, non-peptidic β -secretase inhibitor. *J. Neurosci.* **2011**, *31*, 16507–16516.
- (21) Tresadern, G.; Delgado, F.; Delgado, O.; Gijzen, H.; Macdonald, G. J.; Moechars, D.; Rombouts, F.; Alexander, R.; Spurlino, J.; Van Gool, M.; Vega, J. A.; Trabanco, A. A. Rational design and synthesis of aminopiperazinones as beta-secretase (BACE) inhibitors. *Bioorg. Med. Chem. Lett.* **2011**, *21*, 7255–7260.
- (22) Swahn, B.; Kolmodin, K.; Karlström, S.; von Berg, S.; Söderman, P.; Holenz, J.; Berg, S.; Lindström, J.; Sundström, M.; Turek, D.; Kihlström, J.; Slivo, C.; Andersson, L.; Pyring, D.; Rotticci, D.; Öhberg, L.; Kers, A.; Bogar, K.; Bergh, M.; Olsson, L.; Janson, J.; Eketjäll, S.; Georgievskaja, B.; Jeppsson, F.; Fälting, J. Design and synthesis of β -secretase (bace1) inhibitors with in vivo brain reduction of β -amyloid peptides. *J. Med. Chem.* [Online early access]. DOI: 10.1021/jm3009025. Published Online: Aug 27, 2012.
- (23) Cumming, J. N.; Smith, E. M.; Wang, L.; Misiaszek, J.; Durkin, J.; Pan, J.; Iserloh, U.; Wu, Y.; Zhu, Z.; Strickland, C.; Voigt, J.; Chen, X.; Kennedy, M. E.; Kuvelkar, R.; Hyde, L. A.; Cox, K.; Favreau, L.; Czarniecki, M. F.; Greenlee, W. J.; McKittrick, B. A.; Parker, E. M.; Stamford, A. W. Structure based design of iminohydantoin BACE1 inhibitors: identification of an orally available, centrally active BACE1 inhibitor. *Bioorg. Med. Chem. Lett.* **2012**, *22*, 2444–2449.
- (24) Weiss, M. M.; Williamson, T.; Babu-Khan, S.; Bartberger, M. D.; Brown, J.; Chen, K.; Cheng, Y.; Citron, M.; Croghan, M. D.; Dineen, T. A.; Esmay, J.; Graceffa, R. F.; Harried, S.; Hickman, D.; Hitchcock, S. A.; Horne, D. B.; Huang, H.; Imbeah-Ampiah, R.; Judd, T.; Kaller, M. R.; Kreiman, C. R.; La, D. S.; Li, V.; Lopez, P.; Louie, S.; Monenschein, H.; Nguyen, T. T.; Pennington, L. D.; Rattan, C.; San, M. T.; Sickmier, E. A.; Wahl, R. C.; Wen, P. H.; Wood, S.; Xue, Q.; Yang, B. H.; Patel, V. F.; Zhong, W. Design and preparation of a potent series of hydroxyethylamine containing beta-secretase inhibitors that demonstrate robust reduction of central ss-amyloid. *J. Med. Chem.* **2012**, *55*, 6243–6644.
- (25) Rueeger, H.; Lueoend, R.; Rogel, O.; Rondeau, J.; Mobitz, H.; Machauer, R.; Jacobson, L.; Staufenbiel, M.; Desrayaud, S.; Neumann, U. Discovery of cyclic sulfone hydroxyethylamines as potent and selective β -site APP-cleaving enzyme 1 (BACE1) inhibitors: structure-based design and in vivo reduction of amyloid β -peptides. *J. Med. Chem.* **2012**, *55*, 3364–3386.
- (26) Chang, W. P.; Huang, X.; Downs, D.; Cirrito, J. R.; Koelsch, G.; Holtzman, D. M.; Ghosh, A. K.; Tang, J. Beta-secretase inhibitor GRL-8234 rescues age-related cognitive decline in APP transgenic mice. *FASEB J.* **2011**, *25*, 775–784.
- (27) Edwards, P. D.; Albert, J. S.; Sylvester, M.; Aharony, D.; Andisik, D.; Callaghan, O.; Campbell, J. B.; Carr, R. A.; Chessari, G.; Congreve, M.; Frederickson, M.; Folmer, R. H. A.; Geschwindner, S.; Koether, G.; Kolmodin, K.; Krumrine, J.; Mauger, R. C.; Murray, C. W.; Olsson, L.; Patel, S.; Spear, N.; Tian, G. Application of fragment-based lead generation to the discovery of novel, cyclic amidine β -secretase inhibitors with nanomolar potency, cellular activity, and high ligand efficiency. *J. Med. Chem.* **2007**, *50*, 5912–5925.
- (28) White, R.; Amegadzie, A.; Bryan, M. C.; Chen, J. J.; Cheng, A. C.; Dineen, T.; Epstein, O.; Gore, V. K.; Hua, Z.; Human, J. B.; Huang, H.; Kreiman, C.; La, D.; Liu, Q.; Ma, V. V.; Marx, I.; Patel, V. F.; Qian, W.; Weiss, M.; Yuan, C. C. WO2010030954A1, 2010.
- (29) Takahashi, H.; Fukumoto, H.; Maeda, R.; Terauchi, J.; Kato, K.; Miyamoto, M. Ameliorative effects of a non-competitive BACE1 inhibitor TAK-070 on A β peptide levels and impaired learning behavior in aged rats. *Brain Res.* **2010**, *1361*, 146–156.
- (30) Fukumoto, H.; Takahashi, H.; Tarui, N.; Matsui, J.; Tomita, T.; Hirode, M.; Sagayama, M.; Maeda, R.; Kawamoto, M.; Hirai, K.; Terauchi, J.; Sakura, Y.; Kakihana, M.; Kato, K.; Iwatsubo, T.; Miyamoto, M. A noncompetitive BACE1 inhibitor TAK-070 ameliorates A β pathology and behavioral deficits in a mouse model of Alzheimer's disease. *J. Neurosci.* **2010**, *30*, 11157–11166.
- (31) Malamas, M. S.; Robichaud, A.; Erdei, J.; Quagliato, D.; Solvibile, W.; Zhou, P.; Morris, K.; Turner, J.; Wagner, E.; Fan, K.;

Olland, A.; Jacobsen, S.; Reinhart, P.; Riddell, D.; Pangalos, M. Design and synthesis of aminohydantoinas as potent and selective human β -secretase (BACE1) inhibitors with enhanced brain permeability. *Bioorg. Med. Chem. Lett.* **2010**, *20*, 6597–6605.

(32) Roden, D. M. Drug-induced prolongation of the QT interval. *N. Engl. J. Med.* **2004**, *350*, 1013–1022.

(33) Ekins, S.; Crumb, W. J.; Sarazan, R. D.; Wikel, J. H.; Wrighton, S. A. Three-dimensional quantitative structure–activity relationship for inhibition of human ether-a-go-go-related gene potassium channel. *J. Pharmacol. Exp. Ther.* **2002**, *301*, 427–434.

(34) Diller, J. D. In silico hERG modelling: challenges and progress. *Curr. Comput.-Aided Drug Des.* **2009**, *5*, 106–121.

(35) Asinger, F.; Schaefer, W.; Baumgarte, G.; Mueting, P. F. Concomitant action of elementary sulfur and gaseous ammonia on ketones. XXXVI. Action of sulfur and ammonia on acetophenone. II. Synthesis of 3-imidazoline-5-thiones. *Ann.* **1963**, *661*, 95–110.

(36) Asinger, F.; Saus, A.; Offermanns, H.; Hahn, H. D. Concomitant action of elementary sulfur and gaseous ammonia on ketones. LII. Synthesis of α -oxo thio amides and substituted 3-imidazoline-5-thiones. *Justus Liebigs Ann. Chem.* **1966**, *691*, 92–108.

(37) Asinger, F.; Schaefer, W.; Haaf, F. Concomitant action of elementary sulfur and gaseous ammonia on ketones. XXXVIII. Action of sulfur and ammonia on acetophenone. 3. Proof of structure and reactions of Δ -3-imidazoline-5-thiones. *Justus Liebigs Ann. Chem.* **1964**, *672*, 134–155.

(38) Blid, J.; Ginman, T.; Gravenfors, Y.; Karlstroem, S.; Kihlstrom, J.; Kolmodin, K.; Lindstroem, J.; Rahm, F.; Sundstroem, M.; Swahn, B.; Viklund, J.; von Berg, S.; von Kieseritzky, F. WO 2011/002408 A1, 2011.

(39) Blid, J.; Ginman, T.; Gravenfors, Y.; Karlstroem, S.; Kolmodin, K.; Lindstroem, J.; Plobeck, N.; Rahm, F.; Swahn, B.; Viklund, J.; von Berg, S.; von Kieseritzky, D. WO 2011/002407 A1, 2011.

(40) Lombardo, F.; Shalaeva, M. Y.; Tupper, K. A.; Gao, F. ElogDoct: a tool for lipophilicity determination in drug discovery. 2. Basic and neutral compounds. *J. Med. Chem.* **2001**, *44*, 2490–2497.

(41) Bridgland-Taylor, M. H.; Hargreaves, A. C.; Easter, A.; Orme, A.; Henthorn, D. C.; Ding, M.; Davis, A. M.; Small, B. G.; Heapy, C. G.; Abi-Gerges, N.; Persson, F.; Jacobson, I.; Sullivan, M.; Albertson, N.; Hammond, T. G.; Sullivan, E.; Valentin, J. P.; Pollard, C. E. Optimisation and validation of a medium-throughput electrophysiology-based hERG assay using IonWorks HT. *J. Pharmacol. Toxicol. Methods* **2006**, *54*, 189–199.

(42) Wan, H.; Holmen, A.; Nagard, M.; Lindberg, W. Rapid screening of pK_a values of pharmaceuticals by pressure-assisted capillary electrophoresis combined with short-end injection. *J. Chromatogr., A* **2002**, *979*, 369–377.

(43) Wan, H.; Holmen, A. G.; Wang, Y.; Lindberg, W.; Englund, M.; Nagard, M. B.; Thompson, R. A. High-throughput screening of pK_a values of pharmaceuticals by pressure-assisted capillary electrophoresis and mass spectrometry. *Rapid Commun. Mass Spectrom.* **2003**, *17*, 2639–2648.

(44) Alelyunas, Y. W.; Liu, R.; Pelosi-Kilby, L.; Shen, C. Application of a dried-DMSO rapid throughput 24-h equilibrium solubility in advancing discovery candidates. *Eur. J. Pharm. Sci.* **2009**, *37*, 172–182.

(45) Hopkins, A. L.; Groom, C. R.; Alex, A. Ligand efficiency: a useful metric for lead selection. *Drug Discovery Today* **2004**, *9*, 430–431.

(46) Stachel, S. J.; Coburn, C. A.; Rush, D.; Jones, K. L. G.; Zhu, H.; Rajapakse, H.; Graham, S. L.; Simon, A.; Katharine, H., M.; Allison, T. J.; Munshi, S. K.; Espeseth, A. S.; Zuck, P.; Colussi, D.; Wolfe, A.; Pietrak, B. L.; Lai, M.; Vacca, J. P. Discovery of aminoheterocycles as a novel β -secretase inhibitor class: pH dependence on binding activity part 1. *Bioorg. Med. Chem. Lett.* **2009**, *19*, 2977–2980.

(47) Waring, M. J.; Johnstone, C. A quantitative assessment of hERG liability as a function of lipophilicity. *Bioorg. Med. Chem. Lett.* **2007**, *17*, 1759–1764.

(48) Denora, N.; Trapani, A.; Laquintana, V.; Lopodota, A.; Trapani, G. Recent advances in medicinal chemistry and pharmaceutical

technology—strategies for drug delivery to the brain. *Curr. Top. Med. Chem. (Sharjah, United Arab Emirates)* **2009**, *9*, 182–196.

(49) Alex, A.; Millan, D. S.; Perez, M.; Wakenhut, F.; Whitlock, G. A. Intramolecular hydrogen bonding to improve membrane permeability and absorption in beyond rule of five chemical space. *MedChemComm* **2011**, *2*, 669–674.

(50) Kuhn, B.; Mohr, P.; Stahl, M. Intramolecular hydrogen bonding in medicinal chemistry. *J. Med. Chem.* **2010**, *53*, 2601–2611.

(51) Patel, S.; Vuillard, L.; Cleasby, A.; Murray, C. W.; Yon, J. Apo and inhibitor complex structures of BACE (beta-secretase). *J. Mol. Biol.* **2004**, *343*, 407–416.

(52) Leslie, A. G. W. Recent changes to the MOSFLM package for processing film and image plate data. *Jt. CCP4 ESF-EAMCB Newsl. Protein Crystallogr.* **1992**, *26*, 27.

(53) Evans, P. Scaling and assessment of data quality. *Acta Crystallogr., Sect. D: Biol. Crystallogr.* **2006**, *D62*, 72–82.

(54) Hong, L.; Koelsch, G.; Lin, X.; Wu, S.; Terzyan, S.; Ghosh, A. K.; Zhang, X. C.; Tang, J. Structure of the protease domain of memapsin 2 (beta-secretase) complexed with inhibitor. *Science* **2000**, *290*, 150–153.

(55) Murshudov, G. N.; Vagin, A. A.; Dodson, E. J. Refinement of macromolecular structures by the maximum-likelihood method. *Acta Crystallogr., Sect. D: Biol. Crystallogr.* **1997**, *53*, 240–255.

(56) Emsley, P.; Cowtan, K. Coot: model-building tools for molecular graphics. *Acta Crystallogr., Sect. D: Biol. Crystallogr.* **2004**, *60*, 2126–2132.

(57) BUSTER, version 2.11.1; Global Phasing Ltd.: Cambridge, U.K., 2010.

(58) Wlodek, S.; Skillman, A. G.; Nicholls, A. Automated ligand placement and refinement with a combined force field and shape potential. *Acta Crystallogr., Sect. D: Biol. Crystallogr.* **2006**, *62*, 741–749.

(59) LeDonne, N. C., Jr.; Rissolo, K.; Bulgarelli, J.; Tini, L. Use of structure–activity landscape index curves and curve integrals to evaluate the performance of multiple machine learning prediction models. *J. Cheminf.* **2011**, *3*, 7.

(60) Friden, M.; Ljungqvist, H.; Middleton, B.; Bredberg, U.; Hammarlund-Udenaes, M. Improved measurement of drug exposure in the brain using drug-specific correction for residual blood. *J. Cereb. Blood Flow Metab.* **2010**, *30*, 150–161.

(61) Borgegard, T.; Jureus, A.; Olsson, F.; Rosqvist, S.; Sabirsh, A.; Rotticci, D.; Paulsen, K.; Klintonberg, R.; Yan, H.; Waldman, M.; Stromberg, K.; Nord, J.; Johansson, J.; Regner, A.; Parpal, S.; Malinowsky, D.; Radesater, A. C.; Li, T.; Singh, R.; Eriksson, H.; Lundkvist, J. First and second generation gamma-secretase modulators (GSMs) modulate amyloid-beta (A β) peptide production through different mechanisms. *J. Biol. Chem.* **2012**, *287*, 11810–11819.

(62) Dayneka, N. L.; Garg, V.; Jusko, W. J. Comparison of four basic models of indirect pharmacodynamic responses. *J. Pharmacokin. Biopharm.* **1993**, *21*, 457–478.